

000
001
002
003
004
005
006
007
008
009
010
011
012
013
014
015
016
017
018
019
020
021
022
023
024
025
026
027
028
029
030
031
032
033
034
035
036
037
038
039
040
041
042
043
044
045
046
047
048
049
050
051
052
053

MERGE-OF-THOUGHT DISTILLATION

Anonymous authors

Paper under double-blind review

ABSTRACT

Efficient reasoning distillation for long chain-of-thought (CoT) models is increasingly constrained by the assumption of a single oracle teacher, despite the practical availability of multiple candidate teachers and growing CoT corpora. We revisit teacher selection and observe that different students have different “best teachers,” and even for the same student, the best teacher can vary across datasets. Therefore, to unify multiple teachers’ reasoning abilities into a student to overcome conflicts among various teachers’ supervision, we propose **Merge-of-Thought Distillation (MoT)**, a lightweight framework that alternates between teacher-specific supervised fine-tuning branches and weight-space merging of the resulting student variants. On competition math benchmarks, using only about 200 CoT samples, applying MoT to a Qwen3-14B student surpasses strong models including Deepseek-R1, Qwen3-32B, and OpenAI-O1, demonstrating substantial gains. Besides, MoT consistently outperforms the best single-teacher distillation, improves general reasoning beyond mathematics while reducing catastrophic forgetting, and shows robustness to distribution-shifted and peer-level teachers. Finally, we have demonstrated MoT possesses consensus CoT by eliminating teacher-specific inductive biases and inter-teacher conflicts while repeatedly reinforcing the learning of consensus reasoning features. These results position MoT as a simple, effective route to efficiently distilling long CoT capabilities from diverse teachers into compact students.

1 INTRODUCTION

As large language models (LLMs) with long chain-of-thought (CoT) capabilities continue to emerge (Jaech et al., 2024; Yang et al., 2025a; Guo et al., 2025), reasoning distillation is becoming the key pathway for converting expensive reasoning ability into deployable efficiency. Compared with imitating only final answers, directly supervising the reasoning trajectory enables a smaller student model to learn multi-step solution procedures (Luo et al., 2025b; Qin et al., 2025; Guo et al., 2025).

Building on these developments, the research focus is shifting from scaling data volume to improving data quality. For example, supervised fine-tuning on only 1,000 teacher-distilled samples delivers measurable reasoning gains when paired with test-time compute (Muennighoff et al., 2025). Likewise, when pretraining already imparts rich mathematical knowledge, a few hundred carefully curated examples can effectively elicit complex reasoning (Ye et al., 2025). Taken together, these findings indicate that efficiently distilling long CoT trajectories is an effective strategy for training compact models that achieve competitive reasoning accuracy.

However, real-world deployments rarely features a “single oracle teacher.” We often have multiple candidate teacher LLMs and a growing pool of distilled CoT data, giving rise to a basic question: ***Given a student model, how we pick the most suitable teacher?*** Empirically, teacher choice matters—the teacher can imprint a recognizable “style signature” on the student (Chen et al., 2025b); mismatches between teacher and student can weaken the transfer of long CoT skills (Wu et al., 2025b). As illustrated in Figure 1, our observations are consistent: different students have different “best teachers,” and even for the same student the best teacher can vary across datasets. Such phenomena challenge the naive assumption that “a bigger/stronger teacher is necessarily better,” prompting us to consider: ***Instead of being constrained by a single teacher and the inherent costs of its selection, a more robust and effective paradigm involves aggregating knowledge from multiple teachers.***

054
 055 A natural follow-up question is: **How can we**
 056 **effectively fuse the diverse strengths of multi-**
 057 **ple teachers?** The goal is to consolidate their
 058 complementary reasoning features into a sin-
 059 gle student. Long CoTs often accumulate noise
 060 and irrelevant content (Luo et al., 2025a; Zhang
 061 et al., 2025; Li et al., 2025b). It is unclear
 062 whether, in mixed-teacher long-CoT distilla-
 063 tion, such noise is amplified through inter-
 064 actions, and how to suppress noise while pre-
 065 serving the consensus features. It suggest that:
Diversity of teachers and reasoning paths is
 066 **an asset—provided we can overcome conflicts**
 067 **among the supervision of various teachers.**

068 As an effective technique for overcoming data distribution conflicts, model merging has been widely
 069 applied to joint training across diverse domains and tasks (Yu et al., 2024b; Zhou et al., 2024; Yadav
 070 et al., 2024). However, our revisiting analysis also showed that a single Post-hoc merge does not
 071 reliably resolve cross-teacher supervision conflicts and unify different teachers’ reasoning abilities.
 072 These limitations motivate an approach that goes beyond one-shot merging to reconcile heteroge-
 073 neous teacher signals by **repeatedly reinforcing the learning of consensus reasoning features.**

074 To this end, we propose **Merge-of-Thought Distillation (MoT)**: a lightweight framework that alter-
 075 nates between (i) **teacher-specific branch SFT** and (ii) **weight-space merging of student variants**.
 076 Intuitively, branch SFT internalizes the reasoning style of each teacher into one student; the subse-
 077 quent parameter-space merge then distills consensus—retaining features reinforced across teachers
 078 while suppressing individual accidents and quirks. After multiple iterations, the student progres-
 079 sively condenses into a merged student that reflects multi-teacher consensus reasoning. We found
 080 that MoT significantly enhanced reasoning ability of the model and alleviated catastrophic for-
 081 getting. In addition, we have experimentally and theoretically demonstrated that **consensus CoT**
 082 **emerges naturally with MoT**: MoT eliminates teacher-specific inductive biases and inter-teacher
 083 conflicts at the token level while repeatedly reinforcing the learning of consensus reasoning features,
 084 enabling training in a flatter loss landscape and effective transfer to new student models.

085 We present, to our knowledge, the **first systematic study of multi-teacher long CoT co-**
 086 **distillation**:

- 087 1. We conduct the revisiting analysis of teacher selection under Long CoT distillation set-
 088 ting and find that there is no single best teacher consistently dominant across students or
 089 datasets.
- 090 2. Rather than taking the cost on teacher selection, we propose a novel distillation method,
Merge-of-Thought Distillation (MoT), to unify multiple teachers’ reasoning abilities into
 091 students by overcoming conflicts among the supervision of various teachers.
- 092 3. Using only about 200 CoT samples, applying MoT to a Qwen3-14B student surpasses
 093 strong models including Deepseek-R1, Qwen3-32B, and OpenAI-O1. Besides, MoT
 094 consistently outperforms the best single-teacher distillation, improves general reason-
 095 ing beyond mathematics while reducing catastrophic forgetting, and shows robustness to
 096 distribution-shifted and peer-level teachers.
- 097 4. We have demonstrated MoT possesses consensus CoT by eliminating teacher-specific in-
 098 ductive biases and inter-teacher conflicts while repeatedly reinforcing the learning of con-
 099 sensus reasoning features, which enables the model to be trained on a flatter loss landscape
 100 and further propagated to new student models.

102 2 RELATED WORK

103 **Long Chain-of-Thought Distillation.** Research on distilling long chains of thought (CoT) has
 104 progressed rapidly (Wu et al., 2025b; Guo et al., 2025). Early work (Li et al., 2023) showed that
 105 even small models can benefit from teacher CoT prompting and highlighted the importance of varied
 106 reasoning chains. Subsequent approaches (Luo et al., 2025b; Feng et al., 2024) further segment

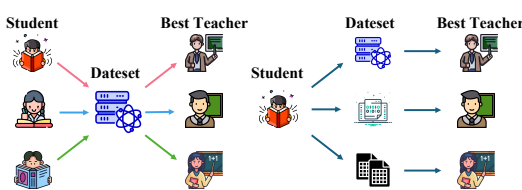


Figure 1: Teacher choice is not universal. Left: different students have different “best teachers”; right: even for the same student the best teacher can vary across datasets. This observation is empirically confirmed in Table 1.

108 and simplify CoTs, employ keypoint weighting, and use progressive distillation to focus on critical
 109 tokens. Studies on the key factors of CoT distillation reveal that teacher diversity and rationale
 110 granularity often have a greater impact than raw teacher accuracy (Chen et al., 2025b). Recent works
 111 also show that long-CoT capability can be bootstrapped with a handful of in-context examples (Pang
 112 et al., 2025), distilled as summaries to improve long-context memory (Ma et al., 2025), or integrated
 113 with vision reasoning using agent-based approaches (Shi et al., 2024). These findings underscore
 114 that long-CoT distillation not only requires carefully curated examples but also faces challenges such
 115 as **teacher selection, noise amplification and distillation efficiency**. Nevertheless, most existing
 116 methods focus on a **single teacher distillation**; our work instead extends this line of work by fusing
 117 multiple teachers’ reasoning abilities into a single student to achieve stronger performance.
 118

119 **Model Merging in LLMs.** Model merging fuses the parameters of multiple trained models into
 120 a single model, which is distinct from output-level ensembles (Yang et al., 2024; Tam et al., 2024).
 121 Empirical studies show that merging tends to balance performance and safety better than mixing data
 122 across tasks or languages (Yang et al., 2025b; Yadav et al., 2024; Yu et al., 2024b; Jin et al.). More
 123 advanced techniques adapt merging to pre-trained models by disentangling weights into magnitude
 124 and direction (Yu et al., 2024a). Other approaches merge checkpoints during pre-training for faster
 125 convergence or use activation importance to retain critical parameters (Li et al., 2025a; Nobari et al.,
 126 2025). Model merging has also been applied to combine models with different reasoning strategies
 127 and to merge heterogeneous architectures (Wu et al., 2025a; Zhang et al., 2024). However, most
 128 existing work focuses on merging models specialised for different domains and tasks; by contrast,
 129 our approach merges student models distilled by different teachers on the same dataset to **unify their**
 130 **reasoning abilities** without conflicts among different teachers.
 131

Table 1: Best teacher under STD for each base model and dataset.

Base model	Best teacher on BOBA-200	Best teacher on S1K-200
Qwen3-8B	QWQ	QWQ
Qwen3-14B	Qwen3-235B	QWQ
Qwen3-30B-A3B	Qwen3-235B	Qwen3-235B

3 REVISITING MULTI-TEACHER LONG CoT DISTILLATION

140 **Setup and goals.** We fine-tune three students from the Qwen3 family (Qwen3-8B / Qwen3-14B /
 141 Qwen3-30B-A3B) on two teacher-distilled math subsets, BOBA-200 and S1K-200. We compare
 142 three regimes: (i) **single-teacher distillation (STD)**, (ii) a **direct multi-teacher union (MTD)** that
 143 mixes all available teacher-distilled samples, and (iii) a **one-shot post-hoc weight merge** of stu-
 144 dents independently distilled from different teachers. Further dataset/model/training details appear
 145 in Sec. 5. This section has two goals: (1) revisit teacher selection under long CoT distillation and
 146 quantify that the best teacher is student and dataset-dependent; and (2) show that naive MTD or a
 147 single *post-hoc* merge does not reliably resolve cross-teacher supervision conflicts.
 148

Table 2: Final AIME24/25 AVG under three regimes. MTD denotes naive multi-teacher union. Best
 149 STD denotes best single-teacher for that setting. MTD and Post-hoc weight merge do not reliably
 150 overcome cross-teacher conflicts or unify heterogeneous reasoning styles.

Base Model	Dataset	Baseline	MTD	Best STD	Post-hoc Merge
Qwen3-8B	BOBA-200	71.46	72.50	71.88	73.12
	S1K-200	71.46	73.23	72.09	73.02
Qwen3-14B	BOBA-200	74.59	75.94	76.98	76.98
	S1K-200	74.59	76.26	76.57	76.26
Qwen3-30B-A3B	BOBA-200	75.77	76.67	78.65	78.54
	S1K-200	75.77	76.46	77.61	77.08

160 **Different students have different best teachers.** Table 1 summarizes, which single-teacher dis-
 161 tillation (STD) source achieves the best distillation performance for each base model and dataset.
 162

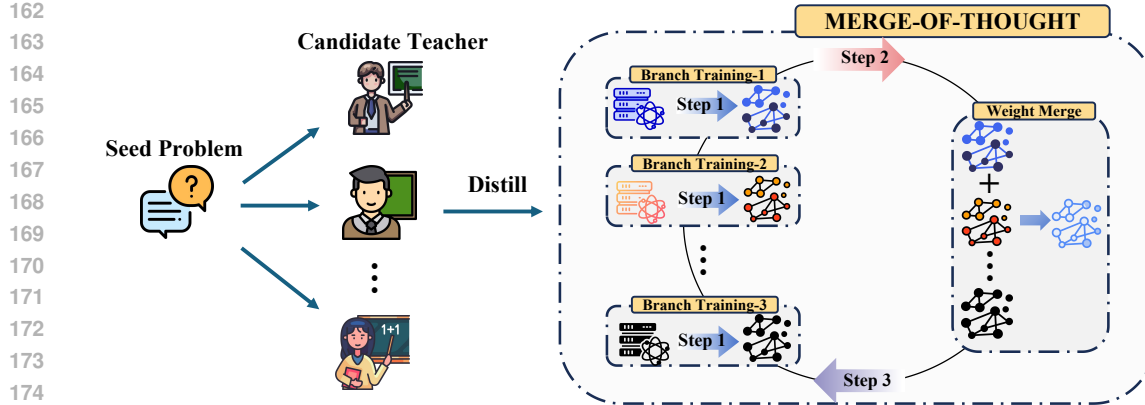


Figure 2: Workflow of Merge-of-Thought Distillation (MoT). After the candidate teachers generate the teacher-specific distillation dataset based on the seed problem, the system enters the iterative MoT algorithm process. In each round t , we perform three steps: **Step 1 (branch training)**: initialize K branches from the current merged student and train each on its teacher-specific distillation dataset $\mathcal{D}^{(k)}$ (Eq. 1); **Step 2 (weight merge)**: average the branch parameters in weight space to obtain the aggregated model $\theta^{(t)}$ (Eq. 2); **Step 3 (next-round initialization)**: use $\theta^{(t)}$ as the base initialization for round $t+1$.

We observe that different students have different best teacher, and **even for the same student the best teacher can vary across datasets**. This revisiting analysis challenges the naive belief that a larger/stronger teacher is always better. Details are provided in the Table 4.

Simple mixing or one-shot post-hoc merging is insufficient. Table 2 reports final AIME24/25 AVG across two datasets and three student scales. While MTD often improves over the base model, it sometimes lags behind the best per-setting STD especially when the scale of the student model grows. In practice, post-hoc merging behaves similarly to MTD. This means that a straightforward MTD that directly unioning all teachers’ distilled samples, and a single post-hoc weight merge of independently distilled students **do not reliably overcome cross-teacher conflicts or unify heterogeneous reasoning styles, motivating the need for an iterative merge-and-train approach** introduced next in Sec. 4 to reconcile heterogeneous teacher signals by repeatedly reinforcing the learning of consensus reasoning features.

4 METHOD: MERGE-OF-THOUGHT DISTILLATION (MoT)

Our approach assumes access to a base language model, a small set of supervised problems with reference answers, and multiple teacher models. The core idea is to consolidate reasoning signals that are consistent across heterogeneous teacher rationales. MoT alternates between teacher-specific supervised fine-tuning (SFT) branches and weight-space merging, and is performed iteratively. Concretely, MoT consists of two core steps repeated for multiple rounds:

1. *Branch training (teacher-specific SFT)*: For each teacher, fine-tune a branch of the student on that teacher’s rationales.

2. *Weight merge*: Merge branch parameters by averaging to form the next student initialization.

We detail the setup and these steps below. An overview of the approach is illustrated in Figure 2.

4.1 INITIALIZATION

Data. Let $\mathcal{D} = \{(x_i, y_i)\}_{i=1}^N$ be a set of problems x with reference answers y . We consider K teacher models. For each input x , teacher τ_k produces a rationale $r^{(k)}$ and a final answer $\hat{y}^{(k)}$. When y is available, we optionally retain only the teacher outputs that match the reference answer, yielding teacher-specific datasets:

$$\mathcal{D}^{(k)} = \{(x_i, r_i^{(k)})\}_{i=1}^{N_k},$$

which filters out teacher trajectories that do not reach the correct final answer.

216 **Model.** Let m denote the student with parameters θ . We initialize from the base model parameters
 217 $\theta^{(0)}$ and iterate the MoT procedure for $t = 1, \dots, T$ rounds.
 218

219 **4.2 TEACHER-SPECIFIC SFT (BRANCH TRAINING)**
 220

221 **Targets.** For each teacher k , we train the student to produce the teacher’s rationale:
 222

$$\text{target}(x; k) = r^{(k)}.$$

224 This choice encourages the student to internalize teacher-specific reasoning patterns, rather than
 225 only the short final answer.
 226

227 **Objective.** The SFT objective for teacher k is the token-level cross-entropy over the target sequence:
 228

$$\mathcal{L}_{\text{SFT}}^{(k)}(\theta) = \mathbb{E}_{(x, r^{(k)}, y) \sim \mathcal{D}^{(k)}} \sum_{t=1}^{L(x, k)} -\log p_{\theta}(z_t | x, z_{<t}), \quad (1)$$

231 where $z_{1:L(x, k)}$ tokenizes $\text{target}(x; k)$. In round t , we initialize K branches from the current merged
 232 model and fine-tune each branch on its teacher’s data:
 233

$$\theta^{(t, k)} \leftarrow \arg \min_{\theta} \mathcal{L}_{\text{SFT}}^{(k)}(\theta) \quad \text{with init } \theta^{(t-1)}.$$

236 **4.3 WEIGHT-SPACE MERGING AND ITERATION**
 237

238 After branch training, we merge the K branch parameters by averaging to get the next initialization:
 239

$$\theta^{(t)} = \frac{1}{K} \sum_{k=1}^K \theta^{(t, k)}. \quad (2)$$

243 This step consolidates reasoning features that are shared across branches while smoothing out
 244 teacher-specific noises. We repeat the two steps—branch training and weight merge—for T rounds,
 245 resulting in the final merged model $\theta^{(T)}$. We aim to leverage *model merging* to overcome conflicts
 246 among various teachers’ supervision and, through continuous merge-and-training iterations, unify
 247 different teachers’ reasoning abilities and ultimately converge to a consensus reasoning landscape.
 248

249 **5 EXPERIMENTS SETUP**
 250

251 **Datasets.** We work in a one-question–multiple-answers (1Q–multiA) setting. We use two high-
 252 quality open-source mathematical datasets (BOBA (inclusionAI, 2025) and S1K (Muennighoff
 253 et al., 2025) as our source datasets. From each source dataset, we sample 200 prompts and
 254 denote the resulting subsets as BOBA-200 and S1K-200. For every prompt, we query four teacher
 255 models—Qwen3-32B (Yang et al., 2025a), QWQ (Team, 2024b), Deepseek-R1 (Guo et al., 2025),
 256 and Qwen3-235B (Yang et al., 2025a). Each teacher generates 16 responses with temperature set to
 257 0.6 and max_tokens set to 32,768. For distillation, we randomly select one correct reasoning path
 258 among the 16 as the training label; if none of the 16 responses is correct, we discard that prompt for
 259 the corresponding teacher’s distillation corpus. We construct two training regimes:
 260 (1) **Single-Teacher Distillation (STD)**, where we build one distilled corpus per teacher.
 261 (2) **Multi-Teacher Distillation (MTD)**, where we aggregate all available distilled samples from all
 262 teachers for each source.

262 The resulting STD and MTD datasets and their sizes are summarized in Table 21. Rows with a
 263 specific teacher correspond to STD, while rows with “ALL TEACHERS” correspond to MTD.

264 **Sampling strategy for BOBA-200 and S1K-200.** Following the general observation that random
 265 sampling can lead to variable prompt difficulty in reasoning tasks (Wang et al., 2025b), we adopt
 266 a simple but reproducible sampling strategy for our subsets. For BOBA-200, we directly use the
 267 default 200 problems provided by the official BOBA release, which are themselves obtained by
 268 random sampling from the full benchmark, without any additional filtering or manual selection. For
 269 S1K-200, since some items are proof-style questions (about 200 items) without a verifiable final
 270 answer, we first remove all such problems and then uniformly sample 200 prompts at random from

270 the remaining questions that have a boxed checkable answer. In both cases, we keep the process
 271 as random as possible under the constraint of automatic answer verification and use exactly the
 272 same batch of prompts for all comparative experiments (MoT, all STDs, and MTD) to avoid cherry-
 273 picking and minimize sensitivity to a particular sample.

274 **Training Configuration.** We fine-tune Qwen3-8B, Qwen3-14B, and Qwen3-30-A3B (Yang et al.,
 275 2025a) as base models across all experiments. For MoT, the base model alternates training on each of
 276 the four STD corpora for 50 steps and then performs a merge; this constitutes one merge round. We
 277 run 5 merge rounds in total and report the best-performing round as the final MoT result; For STD
 278 and MTD baselines, to ensure fairness, we train for 250 steps in total and save a checkpoint every 50
 279 steps. We also report the best-performing checkpoint as the final result. More details are provided in
 280 the Appendix G. We evaluate the capabilities of the model in mathematical reasoning using AIME24
 281 (Math-AI, 2024) and AIME25 (Math-AI, 2025). All AIME scores are 16-run averages.

282 Table 3: Main results with MoT on BOBA-200 and S1K-200. “/” denotes an item not reported in
 283 the corresponding baseline’s source. All AIME scores are 16-run averages.

285 Base Model	286 Configuration	287 Annotated Examples	288 AIME24	289 AIME25	290 AVG	291 AVG Gain
292 Qwen3-8B	293 Base	294 —	295 75.83	296 67.08	297 71.46	298 -
	299 DEER (Dai et al., 2025)	300 103K	301 76.70	302 /	303 -	304 -
	305 S-GRPO (Dai et al., 2025)	306 103K	307 77.30	308 /	309 -	310 -
	311 MathSmith-HC (Zhan et al., 2025)	312 11K	313 76.70	314 70.00	315 73.35	316 $\uparrow 1.89$
	317 BOBA-200 + MoT (Ours)	318 200	319 78.33	320 70.63	321 74.48	322 $\uparrow 3.02$
	323 S1K-200 + MoT (Ours)	324 200	325 77.50	326 71.67	327 74.59	328 $\uparrow 3.13$
329 QWEN2.5-14B	330 Base	331 —	332 13.75	333 11.46	334 12.61	335 -
	336 GRPO (Chen et al., 2025a)	337 1K	338 13.33	339 13.13	340 13.23	341 $\uparrow 0.62$
	342 SPO (Chen et al., 2025a)	343 1K	344 14.17	345 16.67	346 15.42	347 $\uparrow 2.81$
	348 RefCritic (SFT) (Tang et al., 2025)	349 10K	350 15.20	351 15.00	352 15.10	353 $\uparrow 2.49$
	354 RefCritic (SFT+RL) (Tang et al., 2025)	355 120K	356 23.00	357 21.20	358 22.10	359 $\uparrow 9.49$
	360 Bespoke-Stratos-17k (Kou et al., 2025)	361 17K	362 20.00	363 13.30	364 16.65	365 $\uparrow 4.04$
	366 Difficulty-Flipped (Kou et al., 2025)	367 17K	368 23.00	369 23.30	370 23.15	371 $\uparrow 10.54$
	374 Long-CoT (Wang et al., 2025a)	375 220K	376 30.00	377 /	378 -	379 -
	382 BOBA-200 + MoT (Ours)	383 200	384 34.17	385 30.00	386 32.09	387 $\uparrow 19.48$
	391 S1K-200 + MoT (Ours)	392 200	393 36.88	394 30.42	395 33.65	396 $\uparrow 21.04$
397 Qwen3-14B	398 Base	399 —	400 79.17	401 70.00	402 74.59	403 -
	404 BOBA-200 + MoT (Ours)	405 200	406 79.38	407 76.88	408 78.13	409 $\uparrow 3.54$
	410 S1K-200 + MoT (Ours)	411 200	412 81.67	413 75.63	414 78.65	415 $\uparrow 4.06$
416 Qwen3-30B-A3B	417 Base	418 —	419 80.63	420 70.90	421 75.77	422 -
	423 UloRL-A3B-32k (Du et al., 2025a)	424 /	425 /	426 73.50	427 -	428 -
	429 S1K-200 + MoT (Ours)	430 200	431 80.83	432 77.50	433 79.17	434 $\uparrow 3.40$
	436 BOBA-200 + MoT (Ours)	437 200	438 82.92	439 78.33	440 80.63	441 $\uparrow 4.86$
442 Qwen3-32B	443 Base	444 —	445 81.46	446 72.08	447 76.77	448 -
	449 Deepseek-R1	450 Base	451 —	452 79.80	453 70.00	454 74.90
456 OpenAI-O1	457 Base	458 —	459 74.30	460 79.20	461 76.75	462 -
	464 OpenAI-O3-MINI	465 Base	466 —	467 79.60	468 74.80	469 77.20

312 6 MULTI-TEACHER DISTILLATION AND MOT YIELD SUBSTANTIAL GAINS

313 6.1 PERFORMANCE ON COMPETITION MATH BENCHMARKS

314 **Main results.** To demonstrate the superiority of MoT, we report gains across multiple model scales
 315 and compare them against two axes of baselines: (i) larger models like Deepseek-R1, Qwen3-32B
 316 and (ii) same-base alternatives trained on methods using substantially larger, differently sourced
 317 reasoning datasets. Because the Qwen3 family is very frontier and lacks extensive public base-
 318 lines, we additionally include results of applying MoT to Qwen2.5-Instruct-14B (Team, 2024a) as a
 319 complementary case to test the effectiveness of MoT on 14B scale.

320 Table 3 reports the final results of MoT on BOBA-200 and S1K-200. For example, “Qwen3-
 321 8B+BOBA-200” denotes Qwen3-8B trained with MoT on BOBA-200 dataset. As shown, **with**
 322 **only 200 training examples** from either BOBA-200 or S1K-200, MoT lifts Qwen3-8B to match

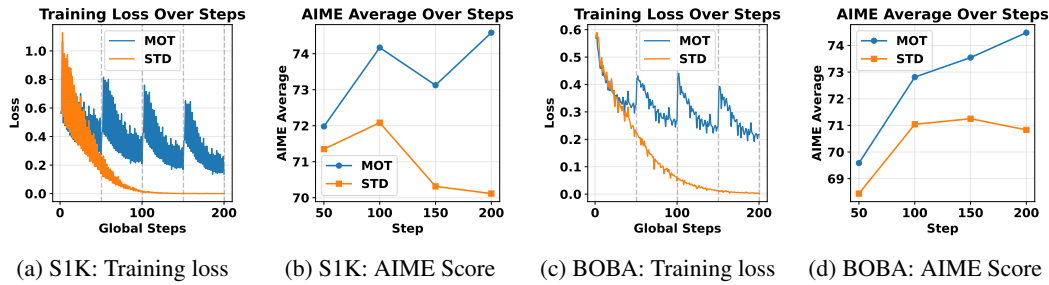
324 the baseline performance of Qwen3-14B. Moreover, MoT on Qwen3-14B surpasses strong models
 325 including Deepseek-R1, Qwen3-32B, and OpenAI-O1, demonstrating substantial gains. In addition,
 326 on Qwen2.5-Instruct-14B, MoT’s improvements far exceed baselines trained on very large reasoning
 327 datasets, reinforcing our claim that **multi-teacher, consensus-based efficient distillation of long**
 328 **CoT reasoning can yield very substantial performance gains.**

329 **Comprehensive Ablations of STD, MTD, and MoT.** To validate the effectiveness of MoT and
 330 multi-teacher distillation, we conduct fine-grained ablations: (1) **STD**: train on each single-teacher
 331 distilled dataset (QWQ, Qwen3-32B, Qwen3-235B, Deepseek-R1). (2) **MTD**: train on the union of
 332 all teachers’ distilled samples. (3) **MoT**: our method that alternates across the four STD corpora
 333 with periodic merges. For fairness, all methods save a checkpoint every 50 steps, and we report the
 334 best checkpoint; full per-step results are provided in the Appendix G.2.

335 Table 4: Ablation on STD, MTD, and MoT across settings. AIME scores are 16-run averages.

Dataset	Method	Qwen3-8B			Qwen3-14B			Qwen3-30B-A3B		
		AIME24	AIME25	AVG	AIME24	AIME25	AVG	AIME24	AIME25	AVG
BOBA	Baseline	75.83	67.08	71.46	79.17	70.00	74.59	80.63	70.90	75.77
	MTD (All Teachers)	76.04	68.96	72.50	76.46	75.42	75.94	79.38	73.96	76.67
	STD (QWQ)	76.25	67.50	71.88	79.58	73.54	76.56	79.79	75.63	77.71
	STD (Qwen3-32B)	75.42	67.71	71.57	77.71	71.25	74.48	81.04	76.04	78.54
	STD (Qwen3-235B)	74.58	67.92	71.25	79.17	74.79	76.98	81.88	75.42	78.65
	STD (Deepseek-R1)	67.71	60.21	63.96	74.38	67.50	70.94	78.33	68.96	73.65
	MoT (ours)	78.33	70.63	74.48	79.38	76.88	78.13	82.92	78.33	80.63
S1K	Baseline	75.83	67.08	71.46	79.17	70.00	74.59	80.63	70.90	75.77
	MTD (All Teachers)	75.63	70.83	73.23	79.17	73.34	76.26	78.33	74.58	76.46
	STD (QWQ)	76.04	68.13	72.09	80.21	72.92	76.57	81.46	72.92	77.19
	STD (Qwen3-32B)	77.50	66.67	72.09	79.79	72.50	76.15	79.58	73.13	76.36
	STD (Qwen3-235B)	74.38	68.54	71.46	77.08	75.41	76.25	79.17	76.04	77.61
	STD (Deepseek-R1)	70.00	61.46	65.73	73.75	62.92	68.34	78.54	70.63	74.59
	MoT (ours)	77.50	71.67	74.59	81.67	75.63	78.65	80.83	77.50	79.17

344 Results are shown in Table 4. MoT consistently yields the strongest distillation gains in almost all
 345 settings, which means that MoT is always superior to the optimal result of the teacher selection
 346 method under each setting. This indicates that MoT can sidestep brittle manual teacher selection
 347 by fusing complementary reasoning abilities into a single student.



361 (a) S1K: Training loss (b) S1K: AIME Score (c) BOBA: Training loss (d) BOBA: AIME Score
 362
 363 Figure 3: Qwen3-8B under MoT vs. STD (QWQ) on *S1K* and *BOBA*. Panels (a,b): S1K; panels
 364 (c,d): BOBA. Left columns show training loss vs. steps; right columns show AIME vs. steps. All
 365 runs log loss at every step on the same QWQ-distilled corpus; AIME is evaluated every 50 steps.

366 **Training Dynamics: MoT vs. Best STD.** We compare Qwen3-8B under MoT and under STD
 367 with the best single teacher (QWQ) on both the *S1K* and *BOBA* datasets. We log training loss
 368 on the same QWQ-distilled corpora at every step and evaluate AIME score every 50 step. From
 369 Figure 3, we observe that MoT achieves substantially higher AIME scores even when its training
 370 loss remains much higher than STD’s at the same step. This suggests that in long CoT training,
 371 lower loss is not necessarily correlated with stronger reasoning ability. Moreover, MoT **exhibits a**
 372 **higher performance ceiling and suppresses overfitting**, with STD typically peaking earlier and
 373 then degrading while MoT remains stable or continues improving as steps increase.

374 6.2 COMPUTE–PERFORMANCE TRADE-OFF.

375 There is an inherent trade-off between computational cost and performance in our setting. For
 376 the main BOBA-200 experiments with Qwen3-8B, the training budgets of STD and MoT can be
 377

378
379
380
381
382
383
384

Table 5: Training budgets of STD and MoT on BOBA-200 with Qwen3-8B.

Method	# branches	steps / branch	rounds	total branch-steps
STD	1	250	1	250
MoT	4	50	5	$4 \times 50 \times 5 = 1000$

385
386
387
Table 6: Equal-compute comparison between MoT and RFT-style single-teacher STD on
AIME24/25 with Qwen3-8B and BOBA-200. All STD variants are trained with 4 CoTs per question
for 1000 steps, matching MoT’s total branch-steps and distinct CoT budget.

Method	AIME24	AIME25	AVG
Base	75.83	67.08	71.46
$4 \times \text{STD (32B)}$	75.21	67.92	71.57
$4 \times \text{STD (QWQ)}$	76.46	69.17	72.82
$4 \times \text{STD (235B)}$	75.83	68.13	71.98
$4 \times \text{STD (R1)}$	70.42	59.58	65.14
MoT (ours)	78.33	70.63	74.48

396
397
398
399
400
summarized as shown in Table 5. However, MoT is designed for the realistic setting where multiple
teachers are available and one wishes to maximally leverage them rather than commit to a single
teacher. In practice, MoT remains highly efficient: it takes only about 6 GPU hours to reproduce
the Qwen3+BOBA-200 training on a single $8 \times \text{H800}$ machine, and this can be further accelerated
by training branches in parallel.

401
402
403
404
405
406
407
To directly assess whether MoT’s gains come purely from increased compute, we ran an additional
experiment following the RFT-style setup (Yuan et al., 2023). For each teacher, we re-distilled the
data by sampling 4 diverse CoT trajectories per question with high temperature, yielding $4 \times 200 =$
 800 rationales per teacher. This matches MoT’s total number of distinct CoT sequences (4 teachers
 $\times 200$ questions $\times 1$ CoT each $= 800$), so the comparison controls for both the total compute and
the amount of distinct CoT supervision. We then performed single-teacher STD for 1000 steps on
the chosen teacher’s 800 CoTs, matching the total branch-steps of MoT:

408
409
(1) **MoT**: 4 branches \times 50 steps/branch \times 5 rounds $= 1000$ branch-steps,
(2) **RFT-style STD**: single teacher, 4 CoTs per question (800 CoTs total), **1000** steps.

410
411
412
We saved a checkpoint every 200 steps and report the best checkpoint. The results on AIME24/25
(Qwen3-8B, BOBA-200) are summarized in Table 6.

413
414
415
416
417
The strongest single-teacher STD configuration in this equal-compute regime remains competitive,
but even with this **strictly matched compute and data budget**, it still underperforms MoT. This in-
dicates that MoT’s gains do not arise merely from using more optimization steps; instead, they come
from jointly leveraging multiple teachers, avoiding brittle teacher selection, and unifying comple-
mentary reasoning signals into a single student, thereby raising the overall reasoning ceiling.

418 6.3 MOT MITIGATES FORGETTING AND STRENGTHENS GENERAL REASONING

420
421
422
423
424
425
426
427
428
To assess whether CoT-style training with MoT affects basic capabilities, we evaluate the final
checkpoints trained by MoT and by STD with the per-setting best teacher (Best STD) against the
Base models on nine benchmarks: CEVAL (CEV) (Seifert et al., 2024), SUPER_GPQA (SG) (Du
et al., 2025b), SIMPLE_QA (SQ) (Wei et al., 2024), IFEVAL (IFE) (Zhou et al., 2023), MMLU_PRO
(MP) (Wang et al., 2024), MMLU_REDUX (MR) (Gema et al., 2025), PhyBench (PB) (Meng et al.,
2024), LiveCodeBench (LCB) (Jain et al., 2024), and GPQA-Diamond (GPQA-D) (Rein et al.,
2024). We group these benchmarks into three categories: **catastrophic-forgetting-sensitive tasks**,
reasoning-knowledge tasks and **pure reasoning tasks**. Detailed descriptions of these tasks and
MoTivations for using and classifying them for evaluation are provided in the Appendix H.

429
430
431
For each configuration, we report raw scores and summarize the average change versus the Base
model within each group: “Avg drop” for catastrophic-forgetting tasks and “Avg gain” for reasoning-
knowledge and pure reasoning tasks. We report the results in Table 7. Compared with training on the
single best teacher, MoT typically yields larger gains on reasoning-knowledge and pure reasoning

432 tasks while incurring smaller declines on catastrophic-forgetting-sensitive tasks. This suggests that
 433 MoT not only **strengthens general reasoning** but also helps **mitigate catastrophic forgetting**. In
 434 Appendix E, we provide a more detailed evaluation.

435
436 Table 7: Impact of Best STD and MoT on general benchmarks. All scores are 16-run averages.

437 438 Dataset	439 Base	440 Config	441 Catastrophic-forgetting-sensitive tasks				442 Reasoning-knowledge tasks				443 Pure reasoning tasks			
			444 CEV	445 SG	446 IFE	447 Avg drop	448 SQ	449 MP	450 MR	451 Avg gain	452 PB	453 LCB	454 GPQA-D	455 Avg gain
439 440 BOBA	441 8B	442 Base	83.58	10.51	83.60	-	32.31	71.42	83.21	-	20.47	55.76	57.77	-
		443 Best STD	83.43	9.97	81.62	↓0.89	33.88	72.00	83.68	↑0.87	22.85	59.88	59.85	↑2.86
		444 MoT	83.73	10.09	82.04	↓0.61	34.44	73.30	84.42	↑1.74	24.07	58.79	60.54	↑3.13
441 442 S1K	443 8B	444 Base	83.58	10.51	83.60	-	32.31	71.42	83.21	-	20.47	55.76	57.77	-
		445 Best STD	83.95	10.18	82.35	↓0.40	32.75	72.24	85.02	↑1.02	22.76	59.47	56.31	↑1.51
		446 MoT	84.32	10.15	83.51	↑0.10	33.56	73.01	84.95	↑1.53	23.37	59.58	59.53	↑2.83
443 444 BOBA	445 14B	446 Base	86.78	10.76	84.69	-	32.61	75.26	85.74	-	28.53	61.41	60.83	-
		447 Best STD	83.73	10.26	82.56	↓1.89	32.17	74.71	86.37	↓0.12	30.61	63.21	63.79	↑2.28
		448 MoT	86.70	10.38	83.51	↓0.55	32.65	75.59	86.53	↑0.39	30.77	63.59	64.26	↑2.62
445 446 S1K	447 14B	448 Base	86.78	10.76	84.69	-	32.61	75.26	85.74	-	28.53	61.41	60.83	-
		449 Best STD	84.25	10.00	84.32	↓1.22	32.49	76.21	86.47	↑0.52	30.41	63.10	63.70	↑2.15
		450 MoT	85.66	10.45	84.42	↓0.57	32.56	76.55	86.68	↑0.73	30.78	64.15	64.11	↑2.76
447 448 BOBA	449 30B	450 Base	85.88	10.66	83.76	-	31.68	75.26	85.81	-	28.57	61.08	59.76	-
		451 Best STD	84.18	10.02	80.44	↓1.89	31.52	75.96	86.04	↑0.26	33.31	61.34	61.81	↑2.35
		452 MoT	86.55	10.52	83.54	↑0.10	32.26	76.21	86.74	↑0.82	33.46	62.54	62.34	↑2.98
449 450 S1K	451 30B	452 Base	85.88	10.66	83.76	-	31.68	75.26	85.81	-	28.57	61.08	59.76	-
		453 Best STD	84.62	10.04	79.74	↓1.97	32.40	75.49	86.67	↑0.60	33.38	63.96	61.46	↑3.13
		454 MoT	86.48	10.14	82.91	↓0.26	33.19	76.49	87.28	↑1.40	33.40	63.92	62.53	↑3.48

451
452
453 7 MOT ENABLES SELECTION-FREE COT DISTILLATION
454

455 **Ablating a Distribution-Shifted Teacher from MoT: Evidence of Complementarity.** As shown
 456 in Table 4, using Deepseek-R1 (R1) as the sole teacher (STD) induces notable performance drops
 457 for QWEN bases, indicating a strong distribution shift. To verify that MoT can still leverage useful
 458 signals from R1 despite the shift, we ablate R1 from the MoT teacher pool and keep all other settings
 459 identical. As shown in Table 8, removing R1 reduces the final MoT performance on BOBA-200
 460 (negative changes), implying that including R1 provides complementary, beneficial supervision that
 461 MoT can harness. This proves that MoT can overcome the **performance degradation** caused by the
 462 strong distribution shift teacher and extract **beneficial common reasoning features** from it. More
 463 details are provided in the Appendix G.3.

464 **Optimization Dynamics with Distribution-Shifted
 465 Teacher.** We visualize optimization dynamics on *BOBA* for both **8B** and **14B** scales under standard MoT and MoT
 466 without R1 (removing the R1 teacher). We log training
 467 loss at every step on the same QWQ-distilled corpus and
 468 evaluate AIME score every 50 steps (as in our ablation
 469 protocol). From Figure 4, we observe that although the
 470 performance of the no-R1 variants converges faster, in-
 471 cluding R1 **raises the performance ceiling, delays sat-
 472 ration and reduces post-peak degradation**, suggesting better regularization and a higher training
 473 upper bound at both scales. This indicates that even with the distribution-shifted teacher, MoT
 474 extracts beneficial common reasoning signals while mitigating teacher-specific noise.

475 **Can peer-level models act as teachers?** We find that teacher usefulness extends beyond strictly
 476 stronger models: distilling Qwen3-30B-A3B from peer-level QWQ or Qwen3-32B improves per-
 477 formance. Combining peer-level trajectories with MoT boosts results further (Appendix G.4).

478
479 8 CONSENSUS COT EMERGES NATURALLY WITH MOT
480

481 **Better student is a better teacher.** To verify that MoT learns higher-quality and more general-
 482 izable chains-of-thought (CoT), we conduct a student-as-teacher experiment. Specifically, we take
 483 models trained on BOBA-200 under three regimes (Base, Best STD and MoT) and use each **as a
 484 teacher** to re-distill on BOBA-200 for a new student model. As shown in Appendix C, when the
 485 teacher itself is a student trained with MoT, it almost always provides the **strongest distillation sig-
 486 nal**, yielding the best downstream student performance. These results indicate that **consensus CoT**

487
488 Table 8: Impact of removing R1 from
489 the MoT teacher pool on BOBA-200.

490 Base model	491 AVG change
492 Qwen3-8B	-0.62
493 Qwen3-14B	-0.21
494 Qwen3-30B-A3B	-0.42

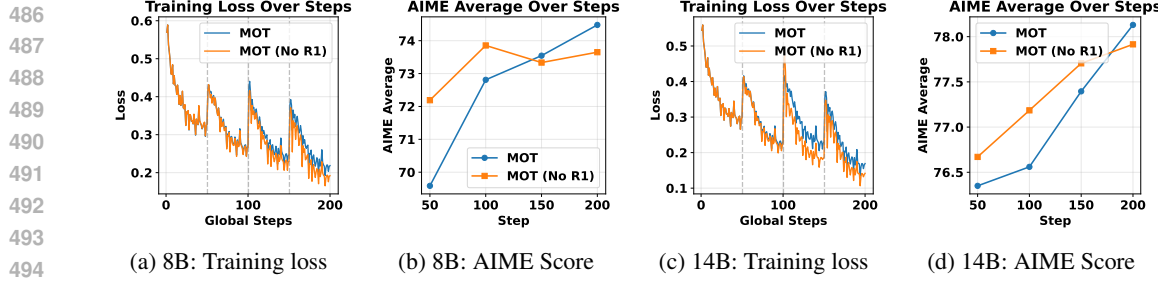


Figure 4: BOBA dataset: MoT vs. MoT without R1 at two scales. Panels (a,b): 8B; panels (c,d): 14B. Left columns show training loss vs. steps; right columns show AIME vs. steps. All runs log loss at every step on the same QWQ-distilled corpus; AIME is evaluated every 50 steps.

emerges naturally with MoT: the student learns trajectories that are both stronger and more consistent, and when used as a teacher, this consensus supervision **transfers** effectively to new students.

Token-level evidence for consensus CoT. We further probe token-level confidence on QWQ-distilled CoTs. We mark tokens for which the MoT model’s output confidence drops relative to the Base under QWQ teacher’s distilled supervision (Figs. 5). Strikingly, the marked tokens concentrate on teacher-specific stylistic expressions (driven discourse markers, hedges, and rhetorical flourishes), whereas core derivational tokens (e.g., operators, equations, intermediate results) retain high confidence. This indicates that MoT is essentially **weakening the learning of inductive bias** of different teachers, while repeatedly **reinforcing the learning of consensus reasoning ability**. We also detail token-level confidence for MoT and STD(R1) on R1-distilled CoTs in the Appendix Figs. 7 and Figs. 8.

Because the three points are A (0 , 0), B (c , 0), C (0 , q). So actually , the triangle is formed by connecting those three points . The area can be calculated as half the determinant :

$$\text{Area} = \frac{1}{2} \times | (A_x (B_y - C_y) + B_x (C_y - A_y) + C_x (A_y - B_y)) | .$$
Plugging in A (0 , 0), B (c , 0), C (0 , q):

$$\text{Area} = \frac{1}{2} \times | 0 * (0 - q) + c * (q - 0) + 0 * (0 - 0) | = (1 / 2) * | c * q | = (1 / 2) c q .$$
Similarly , the area of triangle AD P . Triangle AD P has vertices A (0 , 0), D (0 , d), and P (p , 0). Using the same formula : Area =
$$\frac{1}{2} \times | 0 * (0 - 0) + p * (0 - d) | = (1 / 2) * | - pd | = (1 / 2) pd .$$

Figure 5: Tokens marked with confidence drops relative to the Base model after MoT.

MoT mitigates inter-teacher conflicts and trains in a flatter loss landscape. We design two complementary evaluations with clear goals: (i) a theoretical “two-bonus” decomposition to test whether expert-wise preconditioning boosts the useful driving term and whether cross-teacher interference is provably reduced—thereby explaining conflict mitigation and flatter updates than MTD; and (ii) a linear mode connectivity probe to check loss landscape flatness of MoT. The “two-bonus” decomposition (Appendix A) shows that expert-wise preconditioning of MoT boosts the driving term while a contractive bound reduces cross-teacher interference, with averaging further shrinking the curvature penalty. Complementarily, a linear mode connectivity probe (Appendix D) indicates that MoT yields markedly smoother loss curves than MTD, indicating flatter regions and reduced sensitivity to teacher noises.

9 CONCLUSION

We presented **Merge-of-Thought Distillation** (MoT), a lightweight framework that unifies supervision from multiple heterogeneous teachers for long chain-of-thought (CoT) reasoning by alternating teacher-specific SFT with weight-space merging. Revisiting teacher selection shows that different students have different “best teachers,” and even the same student’s best teacher varies across datasets; MoT sidesteps brittle manual selection by fusing complementary reasoning abilities into a single student. With only about 200 CoT samples, applying MoT to a Qwen3-14B student surpasses Deepseek-R1, Qwen3-32B, and OpenAI-O1. Besides, MoT consistently beats the best single-teacher and naive multi-teacher unions, improves general reasoning while mitigating catastrophic forgetting, and is robust to distribution-shifted and peer-level teachers. Finally, we provide theoretical and empirical evidence that MoT naturally induces a consensus CoT by eliminating teacher-specific inductive biases and inter-teacher conflicts while repeatedly reinforcing the learning of consensus reasoning feature, which enables training in a flatter region of the loss landscape and effective transfer to new student models.

540 **Ethics Statement.** We affirm compliance with the ICLR Code of Ethics. Our study does not
 541 involve human subjects or personally identifiable information. Training/evaluation use public
 542 math/QA benchmarks (e.g., AIM24/25, CEVAL, MMLU variants, GPQA, LiveCodeBench, Phy-
 543 Bench) under their respective licenses; we follow all license terms and cite original sources. Teacher
 544 trajectories (CoTs) are generated by publicly available LLMs and filtered to remove potential toxic-
 545 ity. No sensitive domains (medical/financial/legal advice) are targeted. We report all compute details
 546 to support efficient replication. Any conflicts of interest or sponsorship will be disclosed per ICLR
 547 policy at camera-ready; none are known that would bias the results at submission time.

548 **Reproducibility Statement.** We take reproducibility seriously. The method is fully specified in
 549 Section 4, with training schedules and hyperparameters in Appendix G.1 and ablations in Table 4.
 550 We average AIM2 over 16 seeds and save checkpoints every 50 steps; full per-step results are re-
 551 ported in Appendix G. To facilitate exact reruns, we release (anonymized) artifacts as supplementary
 552 material: main code, training scripts, data preprocessing steps, and environment requirement files
 553 (conda). Appendix 5 details dataset sources, splits, and filtering; Appendix G.1 lists hardware.
 554 These materials allow independent reproduction of tables and figures without additional calibration.

556 REFERENCES

557 Peter Chen, Xiaopeng Li, Ziniu Li, Xi Chen, and Tianyi Lin. Spectral policy optimization: Coloring
 558 your incorrect reasoning in grpo. *arXiv preprint arXiv:2505.11595*, 2025a.

559 Xinghao Chen, Zhijing Sun, Wenjin Guo, Miaoan Zhang, Yanjun Chen, Yirong Sun, Hui Su, Yijie
 560 Pan, Dietrich Klakow, Wenjie Li, et al. Unveiling the key factors for distilling chain-of-thought
 561 reasoning. *arXiv preprint arXiv:2502.18001*, 2025b.

562 Muzhi Dai, Chenxu Yang, and Qingyi Si. S-grpo: Early exit via reinforcement learning in reasoning
 563 models. *arXiv preprint arXiv:2505.07686*, 2025.

564 Jia Deng, Jie Chen, Zhipeng Chen, Daixuan Cheng, Fei Bai, Beichen Zhang, Yinqian Min,
 565 Yanzipeng Gao, Wayne Xin Zhao, and Ji-Rong Wen. From trial-and-error to improvement: A
 566 systematic analysis of llm exploration mechanisms in rlr. 2025. URL <https://arxiv.org/abs/2508.07534>.

567 Dong Du, Shulin Liu, Tao Yang, Shaohua Chen, and Yang Li. Ulorl: An ultra-long output reinforce-
 568 ment learning approach for advancing large language models’ reasoning abilities. *arXiv preprint*
 569 *arXiv:2507.19766*, 2025a.

570 Xinrun Du, Yifan Yao, Kaijing Ma, Bingli Wang, Tianyu Zheng, King Zhu, Minghao Liu, Yiming
 571 Liang, Xiaolong Jin, Zhenlin Wei, et al. Supergpqa: Scaling llm evaluation across 285 graduate
 572 disciplines. *arXiv preprint arXiv:2502.14739*, 2025b.

573 Kaituo Feng, Changsheng Li, Xiaolu Zhang, Jun Zhou, Ye Yuan, and Guoren Wang. Keypoint-
 574 based progressive chain-of-thought distillation for llms. In *Proceedings of the 41st International*
 575 *Conference on Machine Learning*, pp. 13241–13255, 2024.

576 Aryo Pradipta Gema, Joshua Ong Jun Leang, Giwon Hong, Alessio Devoto, Alberto Carlo Maria
 577 Mancino, Rohit Saxena, Xuanli He, Yu Zhao, Xiaotang Du, Mohammad Reza Ghasemi Madani,
 578 et al. Are we done with mmlu? In *Proceedings of the 2025 Conference of the Nations of the Amer-*
 579 *icas Chapter of the Association for Computational Linguistics: Human Language Technologies*
 580 *(Volume 1: Long Papers)*, pp. 5069–5096, 2025.

581 Daya Guo, Dejian Yang, Haowei Zhang, Junxiao Song, Ruoyu Zhang, Runxin Xu, Qihao Zhu,
 582 Shirong Ma, Peiyi Wang, Xiao Bi, et al. Deepseek-r1: Incentivizing reasoning capability in llms
 583 via reinforcement learning. *arXiv preprint arXiv:2501.12948*, 2025.

584 inclusionAI. Areal-boba-data. <https://huggingface.co/datasets/inclusionAI/AREAL-boba-Data>, 2025. URL <https://huggingface.co/datasets/inclusionAI/AREAL-boba-Data>.

594 Aaron Jaech, Adam Kalai, Adam Lerer, Adam Richardson, Ahmed El-Kishky, Aiden Low, Alec
 595 Helyar, Aleksander Madry, Alex Beutel, Alex Carney, et al. Openai o1 system card. *arXiv*
 596 *preprint arXiv:2412.16720*, 2024.

597 Naman Jain, King Han, Alex Gu, Wen-Ding Li, Fanjia Yan, Tianjun Zhang, Sida Wang, Armando
 598 Solar-Lezama, Koushik Sen, and Ion Stoica. Livecodebench: Holistic and contamination free
 599 evaluation of large language models for code. *arXiv preprint arXiv:2403.07974*, 2024.

600 Xisen Jin, Xiang Ren, Daniel Preotiuc-Pietro, and Pengxiang Cheng. Dataless knowledge fusion
 601 by merging weights of language models. In *The Eleventh International Conference on Learning
 602 Representations*.

603 Siqi Kou, Qingyuan Tian, Hanwen Xu, Zihao Zeng, and Zhijie Deng. Which data attributes
 604 stimulate math and code reasoning? an investigation via influence functions. *arXiv preprint
 605 arXiv:2505.19949*, 2025.

606 Liunian Harold Li, Jack Hessel, Youngjae Yu, Xiang Ren, Kai-Wei Chang, and Yejin Choi. Symbolic
 607 chain-of-thought distillation: Small models can also” think” step-by-step. In *The 61st Annual
 608 Meeting Of The Association For Computational Linguistics*, 2023.

609 Yunshui Li, Yiyuan Ma, Shen Yan, Chaoyi Zhang, Jing Liu, Jianqiao Lu, Ziwen Xu, Mengzhao
 610 Chen, Minrui Wang, Shiyi Zhan, et al. Model merging in pre-training of large language models.
 611 *arXiv preprint arXiv:2505.12082*, 2025a.

612 Zihao Li, Xu Wang, Yuzhe Yang, Ziyu Yao, Haoyi Xiong, and Mengnan Du. Feature extrac-
 613 tion and steering for enhanced chain-of-thought reasoning in language models. *arXiv preprint
 614 arXiv:2505.15634*, 2025b.

615 Renjie Luo, Jiaxi Li, Chen Huang, and Wei Lu. Through the valley: Path to effective long cot
 616 training for small language models. *arXiv preprint arXiv:2506.07712*, 2025a.

617 Yijia Luo, Yulin Song, Xingyao Zhang, Jiaheng Liu, Weixun Wang, GengRu Chen, Wenbo Su, and
 618 Bo Zheng. Deconstructing long chain-of-thought: A structured reasoning optimization framework
 619 for long cot distillation. *arXiv preprint arXiv:2503.16385*, 2025b.

620 Junyu Ma, Tianqing Fang, Zhisong Zhang, Hongming Zhang, Haitao Mi, and Dong Yu. Recall with
 621 reasoning: Chain-of-thought distillation for mamba’s long-context memory and extrapolation.
 622 *arXiv preprint arXiv:2505.03320*, 2025.

623 Math-AI. Aime 2024. <https://huggingface.co/datasets/math-ai/aime24>, 2024.
 624 URL <https://huggingface.co/datasets/math-ai/aime24>.

625 Math-AI. Aime 2025. <https://huggingface.co/datasets/math-ai/aime25>, 2025.

626 Fanqing Meng, Wenqi Shao, Lixin Luo, Yahong Wang, Yiran Chen, Quanfeng Lu, Yue Yang, Tian-
 627 shuo Yang, Kaipeng Zhang, Yu Qiao, et al. Phybench: A physical commonsense benchmark for
 628 evaluating text-to-image models. *arXiv preprint arXiv:2406.11802*, 2024.

629 Niklas Muennighoff, Zitong Yang, Weijia Shi, Xiang Lisa Li, Li Fei-Fei, Hannaneh Hajishirzi, Luke
 630 Zettlemoyer, Percy Liang, Emmanuel Candès, and Tatsunori Hashimoto. s1: Simple test-time
 631 scaling. *arXiv preprint arXiv:2501.19393*, 2025.

632 Amin Heyrani Nobari, Kaveh Alimohammadi, Ali ArjomandBigdeli, Akash Srivastava, Faez
 633 Ahmed, and Navid Azizan. Activation-informed merging of large language models. *arXiv
 634 preprint arXiv:2502.02421*, 2025.

635 Bo Pang, Hanze Dong, Jiacheng Xu, Silvio Savarese, Yingbo Zhou, and Caiming Xiong.
 636 Bolt: Bootstrap long chain-of-thought in language models without distillation. *arXiv preprint
 637 arXiv:2502.03860*, 2025.

638 Zeyu Qin, Qingxiu Dong, Xingxing Zhang, Li Dong, Xiaolong Huang, Ziyi Yang, Mahmoud
 639 Khademi, Dongdong Zhang, Hany Hassan Awadalla, Yi R Fung, et al. Scaling laws of synthetic
 640 data for language models. *arXiv preprint arXiv:2503.19551*, 2025.

648 David Rein, Betty Li Hou, Asa Cooper Stickland, Jackson Petty, Richard Yuanzhe Pang, Julien Di-
 649 rani, Julian Michael, and Samuel R Bowman. Gpqa: A graduate-level google-proof q&a bench-
 650 mark. In *First Conference on Language Modeling*, 2024.

651 Christin Seifert, Jörg Schütterer, et al. Ceval: A benchmark for evaluating counterfactual text
 652 generation. In *Proceedings of the 17th International Natural Language Generation Conference*,
 653 pp. 55–69, 2024.

654 Yudi Shi, Shangzhe Di, Qirui Chen, and Weidi Xie. Enhancing video-lm reasoning via agent-of-
 655 thoughts distillation. *arXiv preprint arXiv:2412.01694*, 2024.

656 Derek Tam, Margaret Li, Prateek Yadav, Rickard Brüel Gabrielsson, Jiacheng Zhu, Kristjan Gree-
 657 newald, Mikhail Yurochkin, Mohit Bansal, Colin Raffel, and Leshem Choshen. Llm merging:
 658 Building llms efficiently through merging. In *NeurIPS 2024 Competition Track*, 2024.

659 Qiaoyu Tang, Hao Xiang, Le Yu, Bowen Yu, Hongyu Lin, Yaojie Lu, Xianpei Han, Le Sun, and
 660 Junyang Lin. Refcritic: Training long chain-of-thought critic models with refinement feedback.
 661 *arXiv preprint arXiv:2507.15024*, 2025.

662 Qwen Team. Qwen2. 5: A party of foundation models, 2024a.

663 Qwen Team. Qwq: Reflect deeply on the boundaries of the unknown. *Hugging Face*, 2024b.

664 Yibo Wang, Li Shen, Huanjin Yao, Tiansheng Huang, Rui Liu, Naiqiang Tan, Jiaxing Huang, Kai
 665 Zhang, and Dacheng Tao. R1-compress: Long chain-of-thought compression via chunk compres-
 666 sion and search. *arXiv preprint arXiv:2505.16838*, 2025a.

667 Yiping Wang, Qing Yang, Zhiyuan Zeng, Liliang Ren, Liyuan Liu, Baolin Peng, Hao Cheng, Xuehai
 668 He, Kuan Wang, Jianfeng Gao, Weizhu Chen, Shuohang Wang, Simon Shaolei Du, and Yelong
 669 Shen. Reinforcement learning for reasoning in large language models with one training example,
 670 2025b. URL <https://arxiv.org/abs/2504.20571>.

671 Yubo Wang, Xueguang Ma, Ge Zhang, Yuansheng Ni, Abhranil Chandra, Shiguang Guo, Weiming
 672 Ren, Aaran Arulraj, Xuan He, Ziyan Jiang, et al. Mmlu-pro: A more robust and challenging multi-
 673 task language understanding benchmark. *Advances in Neural Information Processing Systems*,
 674 37:95266–95290, 2024.

675 Jason Wei, Nguyen Karina, Hyung Won Chung, Yunxin Joy Jiao, Spencer Papay, Amelia Glaese,
 676 John Schulman, and William Fedus. Measuring short-form factuality in large language models.
 677 *arXiv preprint arXiv:2411.04368*, 2024.

678 Han Wu, Yuxuan Yao, Shuqi Liu, Zehua Liu, Xiaojin Fu, Xiongwei Han, Xing Li, Hui-Ling Zhen,
 679 Tao Zhong, and Mingxuan Yuan. Unlocking efficient long-to-short lm reasoning with model
 680 merging. *arXiv preprint arXiv:2503.20641*, 2025a.

681 Xiaojun Wu, Xiaoguang Jiang, Huiyang Li, Jucai Zhai, Dengfeng Liu, Qiaobo Hao, Huang Liu,
 682 Zhiguo Yang, Ji Xie, Ninglun Gu, et al. Beyond scaling law: A data-efficient distillation frame-
 683 work for reasoning. *arXiv preprint arXiv:2508.09883*, 2025b.

684 Prateek Yadav, Tu Vu, Jonathan Lai, Alexandra Chronopoulou, Manaal Faruqui, Mohit Bansal,
 685 and Tsendsuren Munkhdalai. What matters for model merging at scale? *arXiv preprint*
 686 *arXiv:2410.03617*, 2024.

687 An Yang, Anfeng Li, Baosong Yang, Beichen Zhang, Binyuan Hui, Bo Zheng, Bowen Yu,
 688 Chang Gao, Chengan Huang, Chenxu Lv, et al. Qwen3 technical report. *arXiv preprint*
 689 *arXiv:2505.09388*, 2025a.

690 Enneng Yang, Li Shen, Guibing Guo, Xingwei Wang, Xiaochun Cao, Jie Zhang, and Dacheng Tao.
 691 Model merging in llms, mllms, and beyond: Methods, theories, applications and opportunities.
 692 *arXiv preprint arXiv:2408.07666*, 2024.

693 Jinluan Yang, Dingnan Jin, Anke Tang, Li Shen, Didi Zhu, Zhengyu Chen, Ziyu Zhao, Daixin Wang,
 694 Qing Cui, Zhiqiang Zhang, et al. Mix data or merge models? balancing the helpfulness, honesty,
 695 and harmlessness of large language model via model merging. *arXiv preprint arXiv:2502.06876*,
 696 2025b.

702 Yixin Ye, Zhen Huang, Yang Xiao, Ethan Chern, Shijie Xia, and Pengfei Liu. Limo: Less is more
 703 for reasoning. *arXiv preprint arXiv:2502.03387*, 2025.
 704

705 Le Yu, Bowen Yu, Haiyang Yu, Fei Huang, and Yongbin Li. Extend model merging from
 706 fine-tuned to pre-trained large language models via weight disentanglement. *arXiv preprint*
 707 *arXiv:2408.03092*, 2024a.

708 Le Yu, Bowen Yu, Haiyang Yu, Fei Huang, and Yongbin Li. Language models are super mario: Ab-
 709 sorbing abilities from homologous models as a free lunch. In *Forty-first International Conference*
 710 *on Machine Learning*, 2024b.

711 Zheng Yuan, Hongyi Yuan, Chengpeng Li, Guanting Dong, Keming Lu, Chuanqi Tan, Chang Zhou,
 712 and Jingren Zhou. Scaling relationship on learning mathematical reasoning with large language
 713 models, 2023. URL <https://arxiv.org/abs/2308.01825>.

714

715 Shaoxiong Zhan, Yanlin Lai, Ziyu Lu, Dahua Lin, Ziqing Yang, and Fei Tang. Mathsmith: Towards
 716 extremely hard mathematical reasoning by forging synthetic problems with a reinforced policy.
 717 *arXiv preprint arXiv:2508.05592*, 2025.

718 Ruiqi Zhang, Changyi Xiao, and Yixin Cao. Long or short cot? investigating instance-level switch
 719 of large reasoning models. *arXiv preprint arXiv:2506.04182*, 2025.

720

721 Yiming Zhang, Baoyi He, Shengyu Zhang, Yuhao Fu, Qi Zhou, Zhijie Sang, Zijin Hong, Kejing
 722 Yang, Wenjun Wang, Jianbo Yuan, et al. Unconstrained model merging for enhanced llm reason-
 723 ing. *arXiv preprint arXiv:2410.13699*, 2024.

724 Jeffrey Zhou, Tianjian Lu, Swaroop Mishra, Siddhartha Brahma, Sujoy Basu, Yi Luan, Denny
 725 Zhou, and Le Hou. Instruction-following evaluation for large language models. *arXiv preprint*
 726 *arXiv:2311.07911*, 2023.

727

728 Yuyan Zhou, Liang Song, Bingning Wang, and Weipeng Chen. Metagpt: Merging large language
 729 models using model exclusive task arithmetic. *arXiv preprint arXiv:2406.11385*, 2024.

730

731

732

733

734

735

736

737

738

739

740

741

742

743

744

745

746

747

748

749

750

751

752

753

754

755

756 **A THEORETICAL ANALYSIS**
 757

758 In this section, we will provide a detailed theoretical analysis to explain the advantages of MoT over
 759 MTD in addressing conflicts and mitigating forgetting issues.
 760

761 Our analysis is based on a comparison of **the gradient update processes of MoT and MTD**.
 762

763 **Preliminary.** We approximate the model update for each expert by using second-order Taylor
 764 expansion:

$$765 \ell_k(\theta) \approx \ell_k(\theta_{t-1}) + g_k^\top(\theta - \theta_{t-1}) + \frac{1}{2}(\theta - \theta_{t-1})^\top H_k(\theta - \theta_{t-1}),$$

766 where $g_k = \nabla \ell_k(\theta_{t-1})$, $H_k = \nabla^2 \ell_k(\theta_{t-1})$, and $\ell_k(\theta)$ is the loss function for expert k evaluated
 767 at point θ . We also define the mixture gradient and Hessian as weighted sums of the individual
 768 gradients and Hessians:
 769

$$770 \bar{g} = \sum_k \alpha_k g_k, \quad \bar{H} = \sum_k \alpha_k H_k,$$

772 where $\alpha_k \geq 0$ and $\sum_k \alpha_k = 1$ are the weights assigned to each expert.
 773

774 Each branch performs E_k steps of gradient descent with a stepsize η starting from θ_{t-1} . Based on
 775 second-order Taylor expansion, we have $\theta_{k,E} = \theta_{t-1} - P_k g_k$, $P_k = \eta \sum_{e=0}^{E-1} (I - \eta H_k)^e$,
 776 where P_k is the ‘‘preconditioner’’ used in each branch’s local optimization process.
 777

We also have the below closed-form solution for preconditioner:
 778

$$779 P_k = s_{E_k}(H_k), \quad s_E(\lambda) = \frac{1 - (1 - \eta\lambda)^E}{\lambda} = \eta \sum_{e=0}^{E-1} (1 - \eta\lambda)^e,$$

782 where $s_E(\lambda)$ represents the effective step size along the direction defined by the eigenvalue λ of the
 783 Hessian matrix H_k .
 784

The expression for $s_E(\lambda)$ can be derived by considering the update rule for gradient descent in the
 785 presence of a Hessian, where each step of gradient descent applies a scaling factor depending on the
 786 eigenvalue λ of the Hessian matrix at each iteration. For large E or small $\eta\lambda$, $s_E(\lambda)$ approximates
 787 the inverse of the eigenvalue λ , leading to more efficient updates along lower-curvature directions.
 788

Hence, the branch displacement for expert k is given by:
 789

$$790 \delta_k = -P_k g_k = -s_{E_k}(H_k) g_k,$$

792 and the MoT merge, which aggregates the displacements from all experts, is:
 793

$$794 \Delta = \sum_k \alpha_k \delta_k = -\sum_k \alpha_k P_k g_k.$$

796 For the MTD, which also runs E local steps at the same anchor point, the preconditioner is defined
 797 as:
 798

$$799 P_{\text{mtd}} = s_E(\bar{H}),$$

800 where \bar{H} is the weighted sum of the Hessians of all experts, and the E -step update is:
 801

$$802 -P_{\text{mtd}} \bar{g} = -s_E(\bar{H}) \bar{g}.$$

803 Here, P_{mtd} is the preconditioner used for the mixture of experts, and \bar{g} is the mixture gradient.
 804

805 **Assumption 1** (Local quadratic & stable steps). *Each ℓ_k is C^2 in a neighborhood \mathcal{N} of θ_{t-1} . Let
 806 $H_k = \nabla^2 \ell_k(\theta_{t-1})$ and $L_{\max} = \max_k \lambda_{\max}(H_k)$. We choose a stepsize $\eta \in (0, 2/L_{\max})$ and run
 807 $E_k \geq 1$ local steps whose iterates remain in \mathcal{N} .*
 808

809 **Two bonuses on the linear part.** The one-round improvement under the quadratic surrogate
 $F_Q(\delta) = \bar{g}^\top \delta + \frac{1}{2} \delta^\top \bar{H} \delta$ splits into a *linear* ‘‘driving’’ term and a *quadratic* penalty. For the linear

810 term we have the following variance-type decompositions:
 811

$$\underbrace{\left\| \sum_k \alpha_k P_k g_k \right\|^2}_{\text{MoT linear}} = \underbrace{\sum_k \alpha_k \langle g_k, P_k g_k \rangle}_{\text{expert-wise preconditioning}} - \underbrace{\frac{1}{2} \sum_{i,j} \alpha_i \alpha_j \|P_i g_i - P_j g_j\|^2}_{I_{\text{mot}} \geq 0}, \quad (3)$$

$$\underbrace{\|\bar{g}\|_{P_{\text{mtd}}}^2}_{\text{mtd linear}} = \underbrace{\sum_k \alpha_k \langle g_k, P_{\text{mtd}} g_k \rangle}_{\text{single preconditioner}} - \underbrace{\sum_k \alpha_k \|g_k - \bar{g}\|_{P_{\text{mtd}}}^2}_{I_{\text{mtd}}(P_{\text{mtd}}) \geq 0}, \quad (4)$$

819 where $\|x\|_M^2 = x^\top M x$. Subtracting equation 4 from equation 3 yields the *two-bonus* difference
 820

$$\begin{aligned} \Delta_{\text{lin}} &:= \left\| \sum_k \alpha_k P_k g_k \right\|^2 - \|\bar{g}\|_{P_{\text{mtd}}}^2 \\ &= \underbrace{\sum_k \alpha_k \langle g_k, (P_k - P_{\text{mtd}}) g_k \rangle}_{\text{(A') preconditioning gain}} + \underbrace{I_{\text{mtd}}(P_{\text{mtd}}) - I_{\text{mot}}}_{\text{(B') interference mitigation}}. \end{aligned} \quad (5)$$

827 **When is (A') ≥ 0 ?**

828 **Lemma 1** (Monotonicity of s_E). *For any fixed $E \geq 1$ and $\eta > 0$, $s_E(\lambda) = \eta \sum_{e=0}^{E-1} (1 - \eta \lambda)^e$ is
 829 strictly decreasing in λ on $(0, 2/\eta)$.*

830 If H_k and \bar{H} are (approximately) simultaneously diagonalizable, then $D_k := \langle g_k, (P_k - P_{\text{mtd}}) g_k \rangle =$
 831 $\|g_k\|^2 \sum_r w_{k,r} (s_E(\lambda_{k,r}) - s_E(\bar{\lambda}_r))$, with weights $w_{k,r} = \frac{(q_r^\top g_k)^2}{\|g_k\|^2}$. Hence $D_k \geq 0$ whenever most
 832 weight lies on directions where $\lambda_{k,r} \leq \bar{\lambda}_r$. Aggregating with α_k gives $(\text{A}') \geq 0$.
 833

834 **When is (B') ≥ 0 ? A contractive bound on interference.** Let $\mathcal{S} = \text{span}\{g_i - g_j\}_{i,j}$ be the
 835 disagreement subspace.

836 **Assumption (direction-wise contraction on \mathcal{S}).** There exists $\rho \in (0, 1]$ such that on \mathcal{S} one of the
 837 following equivalent conditions holds:
 838

839 *(Coord.)* H_k and \bar{H} are (approximately) simultaneously diagonalizable on \mathcal{S} with eigenbasis $\{q_r\}$;
 840 let $p_{k,r} = s_E(\lambda_{k,r})$ and $p_{\text{mtd},r} = s_E(\bar{\lambda}_r)$. For all r with $q_r \in \mathcal{S}$,

$$\max_i p_{i,r} \leq \rho p_{\text{mtd},r}.$$

841 *(Basis-free)* For all $v \in \mathcal{S}$ and all k ,

$$\|P_k v\|^2 \leq \rho^2 \|v\|_{P_{\text{mtd}}}^2 \quad (\text{i.e., } v^\top P_k^\top P_k v \leq \rho^2 v^\top P_{\text{mtd}} v).$$

842 The above is natural on high-curvature/disagreement directions because $s_E(\lambda)$ is decreasing in λ :
 843 along directions where at least one expert has directional curvature no smaller than the mixture (a
 844 common empirical pattern), its preconditioning coefficient is smaller, yielding stronger contraction.
 845

846 Under this assumption we have

$$I_{\text{mot}} = \frac{1}{2} \sum_{i,j} \alpha_i \alpha_j \|P_i g_i - P_j g_j\|^2 \leq \rho^2 \frac{1}{2} \sum_{i,j} \alpha_i \alpha_j \|g_i - g_j\|_{P_{\text{mtd}}}^2 = \rho^2 I_{\text{mtd}}(P_{\text{mtd}}). \quad (6)$$

847 Hence $(\text{B}') = I_{\text{mtd}}(P_{\text{mtd}}) - I_{\text{mot}} \geq (1 - \rho^2) I_{\text{mtd}}(P_{\text{mtd}}) \geq 0$.
 848

849 **Implicit shrinkage from averaging enters the quadratic penalty.** With $\Delta = -\sum_k \alpha_k P_k g_k$, the
 850 quadratic penalties satisfy
 851

$$R_{\text{mot}} = \frac{1}{2} \Delta^\top \bar{H} \Delta \leq \frac{1}{2} \lambda_{\max}(\bar{H}) \left(\sum_k \alpha_k \|P_k g_k\|^2 - \underbrace{I_{\text{mot}}}_{\text{shrinkage from averaging}} \right), \quad (7)$$

$$R_{\text{mtd}} = \frac{1}{2} \eta^2 \bar{g}^\top \bar{H} \bar{g} \leq \frac{1}{2} \lambda_{\max}(\bar{H}) \left(\sum_k \alpha_k \|P_{\text{mtd}} g_k\|^2 - I_{\text{mtd}}(P_{\text{mtd}}) \right). \quad (8)$$

852 Note the *minus* interference terms, showing that averaging contracts the update norm and directly
 853 reduces the curvature penalty.
 854

864
 865 Table 9: MoT applied to Llama-3.1-8B-Instruct on Math500 under the BOBA-200 setting. MoT
 866 consistently outperforms all single-teacher STD variants, indicating that MoT is not tied to Qwen-
 867 specific design choices.

Method	Math500 score
Base	49.65
STD (Qwen3-32B)	55.45
STD (QWQ)	55.80
STD (Qwen3-235B)	57.45
STD (Deepseek-R1)	53.80
MoT (ours)	62.65

876 **Net one-round advantage.** Combining equation 5–equation 6 and the penalty bounds yields

$$\underbrace{\Delta_{\text{mot}} - \Delta_{\text{mtd}}}_{\text{MoT minus MTD}} \gtrsim \underbrace{\sum_k \alpha_k \langle g_k, (P_k - P_{\text{mtd}}) g_k \rangle}_{(A')} + \underbrace{(1 - \rho^2) I_{\text{mtd}}(P_{\text{mtd}})}_{(B')} - \frac{1}{2} \lambda_{\max}(\bar{H}) \cdot [\dots],$$

881 where $[\dots]$ gathers the (usually small in the stable regime) difference of squared update norms.
 882 Thus, under gradient/curvature heterogeneity and stable steps, MoT enjoys a larger linear driving
 883 term (A') and smaller interference (B'), while averaging further cuts the quadratic penalty.
 884

885 **Special case $E = 1$ (for reference).** Then $P_k = P_{\text{mtd}} = \eta I$, and equation 5 reduces to the
 886 familiar two-term decomposition

$$\underbrace{\sum_k \alpha_k f_k \|g_k\|^2 - \eta \|\bar{g}\|^2}_{f_k = \eta} = \underbrace{0}_{(A)} + \underbrace{\eta \sum_k \alpha_k \|g_k - \bar{g}\|^2}_{(B) \text{ variance bonus}}.$$

891 **Remark 1** (Implicit proximal effect (Mitigating Forgetting)). *The matrix series identity $P_k =$
 892 $\eta \sum_{e=0}^{E_k-1} (I - \eta H_k)^e$ shows a direction-dependent shrink toward the anchor; in each eigendirection
 893 λ the effective step is $s_E(\lambda)$, **larger for low curvature and smaller for high curvature**, explaining
 894 MoT’s stability without explicit proximal terms.*

895 **Remark 2** (Unified Improvements (Mitigating Conflicts)). *A positive value for both bonus terms
 896 indicates that MoT reduces gradient interference and produces a larger effective update, thereby
 897 improving optimization progress.*

899 A.1 ADDITIONAL ANALYSES: GENERALIZATION AND ROBUSTNESS OF MOT

901 **Generalization to other backbones.** To examine whether MoT is specific to the Qwen family
 902 or can transfer to other architectures, we replicate the BOBA-200 setup on a different backbone,
 903 **Llama-3.1-8B-Instruct**. We use exactly the same teacher pool, data, and MoT procedure, and
 904 evaluate on Math500. The results are shown in Table 9.

905 MoT significantly improves the Llama-3.1-8B-Instruct backbone and provides a sizable margin over
 906 the *best* single-teacher distillation, supporting the view that MoT is a lightweight, architecture-
 907 agnostic training procedure rather than a Qwen-specific trick.

909 **Seed sensitivity and early stopping.** We further study the robustness of MoT to random seeds
 910 and early-stopping choices. On Qwen3-8B with BOBA-200, we run MoT with 5 independent
 911 seeds under the same 5-round schedule, and report the AIME average (AIME AVG = (AIME24 +
 912 AIME25)/2) at each round. In addition, we implement a fixed validation-based early-stopping rule
 913 for MoT: 10% of the original training set is held out as a validation set, and for each run we select
 914 the checkpoint (across rounds) with the best validation score and then report its test performance.
 915 The results are summarized in Table 10.

916 The peak around merge round 4 is stable across seeds, without any “best-of” checkpoint selection.
 917 Validation-based early stopping yields slightly lower AIME AVG than always using round 4 (as ex-
 918 pected, since the effective training set is smaller), but remains strong and better than any STD/MTD

918
 919 Table 10: MoT robustness across seeds and rounds on Qwen3-8B + BOBA-200. We report AIME
 920 AVG (AIME24/25 average) as mean \pm std over 5 seeds. “Early-stopping” denotes validation-based
 921 selection using a 10% held-out split.

922 Configuration	923 AIME AVG (mean \pm std)
924 Merge round 1	925 70.17 ± 0.63
926 Merge round 2	927 72.37 ± 0.65
928 Merge round 3	929 73.38 ± 0.09
930 Merge round 4	931 74.89 ± 1.05
932 Merge round 5	933 72.75 ± 0.81
934 Early-stopping (val-based)	935 73.46 ± 0.31

936 Table 11: MoT on a code reasoning domain (LiveCodeBench) using 178 code-domain examples.
 937 MoT again outperforms the best single-teacher STD.

938 Method	939 LiveCodeBench score
940 Base	941 55.76
942 STD (32B)	943 58.08
944 STD (QWQ)	945 56.88
946 STD (235B)	947 58.89
948 STD (R1)	949 53.89
950 MoT (ours)	951 61.08

952 baseline, and it also improves over taking the same final checkpoint of MoT without early-stopping.
 953 Overall, these results indicate that MoT’s gains are robust to random seeds and remain effective
 954 under a fixed, validation-based early-stopping rule.

955 **Generalization beyond mathematical reasoning.** To evaluate whether MoT extends beyond
 956 competition math, we consider a code reasoning domain using 178 code-domain examples from
 957 Deng et al. (2025) and apply exactly the same distillation, training, and evaluation pipeline as in the
 958 main experiments (same teacher pool, same 1Q–multiA CoT collection, same MoT procedure). We
 959 evaluate on LiveCodeBench, and report the results in Table 11.

960 As in the mathematical reasoning setting, MoT again outperforms the best single-teacher STD, sug-
 961 gesting that MoT is not restricted to math and can also improve code reasoning under the same
 962 multi-teacher long-CoT setup. Furthermore, as reported in Section 6.3, MoT improves performance
 963 on a range of general benchmarks (e.g., CEVAL, MMLU variants, physics and coding benchmarks)
 964 while incurring smaller drops on catastrophic-forgetting-sensitive tasks compared to the best single-
 965 teacher STD. Together, these results provide concrete evidence that MoT generalizes beyond com-
 966 petition math to other domains and evaluation suites.

967 **Additional math benchmark: HMMT.** To further diversify mathematical evaluation, we also
 968 evaluate Qwen3-8B distilled on BOBA-200 using MoT and four single-teacher STDs on the HMMT
 969 benchmark. Results are shown in Table 12.

970 Here, QWQ remains the best single teacher, consistent with Table 1 for this student/dataset config-
 971 uration, which supports the stability of our teacher-selection analysis under a fixed setting. Impor-
 972 tantly, MoT still achieves the highest score, improving over the best STD and reinforcing that MoT
 973 effectively unifies multiple teachers’ reasoning abilities and raises the student’s reasoning ceiling.

974 **Summary across math and code domains.** Across different evaluation domains—AIME24/25,
 975 HMMT, and the code-reasoning setting—we observe that the identity of the “best” teacher changes
 976 with the dataset or domain (e.g., QWQ vs. Qwen3-235B), supporting our claim that teacher choices
 977 are not universal. At the same time, MoT consistently outperforms all single-teacher STDs in these
 978 settings, confirming the effectiveness of our multi-teacher consensus distillation. A broader sweep

972
 973 Table 12: Performance of Qwen3-8B on HMMT after distillation on BOBA-200. QWQ remains the
 974 strongest single teacher, whereas MoT achieves the best overall score.

Method	HMMT score
Base	38.33
STD (32B)	43.33
STD (QWQ)	48.33
STD (235B)	45.83
STD (R1)	40.83
MoT (ours)	52.50

984
 985 Table 13: Advanced merging baselines and MoT variants on Qwen3-8B + BOBA-200. TIES and
 986 DARE are used both as one-shot merges and as merge operators inside MoT.

Method	AIME AVG
Base	71.46
One-shot TIES	71.67
One-shot DARE	60.42
MoT (TIES)	73.34
MoT (DARE)	74.17
MoT (simple merge, ours)	74.48

996 over additional domains (e.g., large-scale scientific QA) is left for future work, but the new code and
 997 HMMT experiments already provide further evidence beyond the original math benchmarks.

1000 A.2 EFFECT OF MERGING OPERATOR AND NUMBER OF TEACHERS

1001 **Advanced merging operators: TIES and DARE.** To compare MoT against more advanced
 1002 model-merging and data-fusion techniques, we incorporate several recent operators into our
 1003 pipeline. On Qwen3-8B + BOBA-200, we evaluate: (i) one-shot TIES merging, (ii) one-shot DARE
 1004 merging, and (iii) MoT variants that replace simple averaging with TIES or DARE in the merge step.
 1005 All other settings (teachers, data, schedule, evaluation) are kept identical. The final AIME average
 1006 (AIME24/25) is reported in Table 13. We also report the per-round behavior of MoT(TIES) and
 1007 MoT(DARE) in Tables 14 and 15.

1008 These results lead to three observations:

- (1) First, advanced one-shot merges alone are not sufficient in our setting: one-shot TIES brings only a minor gain over the base model, and one-shot DARE causes a severe performance drop. This suggests that techniques designed for merging models trained on different domains or tasks may be much less directly suitable for unifying different reasoning paths for the same questions.
- (2) Second, when TIES or DARE is used inside the MoT loop, performance improves substantially, with DARE gaining almost +14 points over its one-shot counterpart. Algorithmically, this is consistent with the fact that one-shot DARE acts on highly conflicting teacher-specific updates all at once (leading to over-pruning of partially misaligned but useful directions), whereas DARE inside MoT sees smaller, progressively more aligned deltas across rounds and branches, and thus behaves like a gradual consensus regularizer that keeps directions repeatedly reinforced by multiple teachers.
- (3) Third, simple averaging still achieves the highest and most robust ceiling: MoT(TIES) and MoT(DARE) tend to converge faster across rounds but plateau at a slightly lower level or overfit more, while MoT with plain averaging attains the best final AIME AVG. A plausible explanation, consistent with our analysis in Section 7, is that simple averaging does not impose any parameter filtering, allowing MoT to naturally absorb useful signals even from suboptimal or noisy teachers and thereby achieve a higher reasoning ceiling.

1024
 1025 **Effect of the number of teachers.** We also study how MoT behaves as we vary the number of
 teachers. On BOBA-200 with Qwen3-8B, we start from the best single teacher (by STD perfor-

1026

1027

Table 14: MoT(TIES) across merge rounds on Qwen3-8B + BOBA-200.

1028

1029

Round	AIME24	AIME25	AIME AVG
1	73.33	66.67	70.00
2	77.50	67.50	72.50
3	77.50	69.17	73.34
4	74.17	65.00	69.59
5	75.00	65.83	70.42

1030

1031

1032

1033

1034

1035

1036

1037

Table 15: MoT(DARE) across merge rounds on Qwen3-8B + BOBA-200.

1038

1039

1040

1041

1042

1043

1044

1045

1046

1047

mance), then progressively add the second-best, third-best, and finally the noisy teacher R1 into the MoT pool, keeping the MoT configuration fixed. The results are shown in Table 16.

We observe a monotonic improvement in AIME AVG as more teachers are added, and performance continues to increase even after including the distribution-shifted/noisy teacher R1. This supports the view that, in our experimental regime, MoT can effectively extract complementary signals from additional teachers and is robust enough to benefit from them. We do not claim that this behavior will persist for arbitrarily large pools of low-quality or adversarial teachers; in such extreme cases, stronger filtering or adaptive weighting would likely be necessary. Systematically studying how performance scales with larger and more heterogeneous teacher sets is an interesting direction for future work.

B LIMITATIONS

(1) We currently merge branches via simple uniform parameter averaging; future work will explore alternative merge strategies.

(2) Beyond AIME24/25, there is a lack of sufficiently challenging math benchmarks, which limits evaluation depth on high-difficulty mathematical reasoning.

(3) Baseline results in the main results are taken from the original papers/reports because many baselines do not release code/models or disclose key training details like data curation or key hyperparameters. Consequently, they were not re-evaluated under a unified, consistent evaluation configuration, which may affect strict comparability.

C BETTER STUDENT IS A BETTER TEACHER

Table 17: Student-as-teacher distillation on BOBA-200. Teachers are base model or student models obtained with Best-STD/MoT. We report raw scores on reasoning benchmarks mentioned earlier.

Teacher model	Student model	Teacher Config	AIME24	AIME25	PhyBench	LiveCodeBench	GPQA-Diamond	AVG
Qwen3-14B	Qwen3-8B	Base	74.17	67.08	23.06	58.98	57.80	56.22
		Best STD	75.21	64.17	23.74	56.74	58.33	55.64
		MoT	75.63	68.96	24.28	58.83	59.22	57.38
Qwen3-30B-A3B	Qwen3-14B	Base (Vanilla)	79.17	68.96	28.31	61.41	61.65	59.90
		Best STD	77.08	71.88	29.40	63.36	61.87	60.72
		MoT	80.00	71.67	29.63	62.99	62.69	61.40

1080

1081 Table 16: Effect of the number of teachers in MoT on Qwen3-8B + BOBA-200. Teachers are
1082 added in descending order of single-teacher STD performance, with R1 being the most distribution-
1083 shifted/noisy teacher.

1084

1085

1086

1087

1088

1089

1090

1091

1092

1093

1094

1095

1096

1097

1098

1099

1100

1101

1102

1103

1104

1105

1106

1107

1108

1109

1110

1111

1112

1113

1114

1115

1116

1117

1118

1119

1120

1121

1122

1123

1124

1125

1126

1127

1128

1129

1130

1131

1132

1133

# Teachers in MoT	AIME24	AIME25	AIME AVG
1 (best teacher)	76.25	67.50	71.88
2	77.50	68.33	72.92
3	78.13	69.17	73.65
4 (with R1)	78.33	70.63	74.48

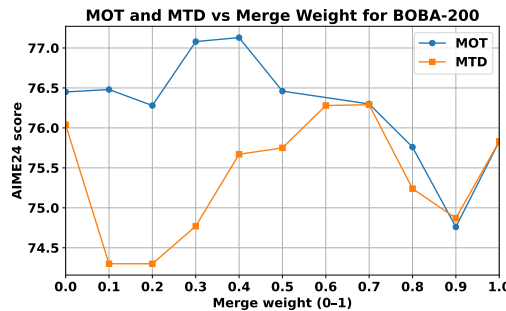
D PROBING LOSS-LANDSCAPE FLATNESS VIA BASE-TO-CHECKPOINT INTERPOLATION: MoT vs. MTD

Setup and purpose. To assess how stably a trained model sits in parameter space, we probe **loss-landscape flatness** via linear mode connectivity (LMC) between the *base* model and the final trained checkpoint (from either MTD or our MoT). For $\lambda \in [0, 1]$, we define

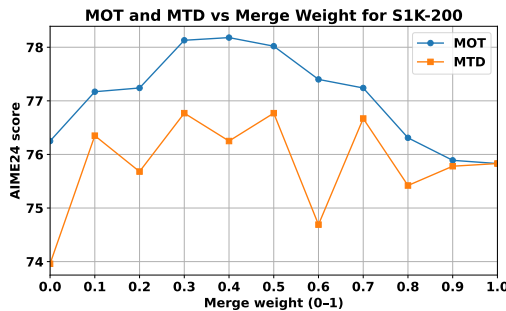
$$\theta(\lambda) = \lambda \theta_{\text{base}} + (1 - \lambda) \theta_{\text{ckpt}},$$

so that $\lambda=1$ recovers the base model and $\lambda=0$ recovers the trained checkpoint. At each λ on a fixed grid, we evaluate AIME24 (pass@1, 64-run average). A smooth/high trajectory indicates a flatter, more robust region with fewer barriers; a sharp/erratic trajectory suggests a bumpier landscape and stronger interference among supervision signals.

Findings. On both BOBA-200 and S1K-200 with the 8B student, MoT yields a **much smoother** and more stable performance curve than MTD as λ varies: performance rises steadily toward the checkpoint and decays gradually away from it. This behavior is consistent with MoT training in a **flatter** region (greater robustness to weight perturbations) and **better reconciliation of cross-teacher supervision conflicts**. In contrast, MTD exhibits steeper drops and local irregularities, implying residual inter-teacher interference.



(a) Qwen3-8B on BOBA-200.



(b) Qwen3-8B on S1K-200.

Figure 6: Base-to-checkpoint linear interpolation (LMC). MoT shows smoother, higher trajectories than MTD on AIME24, indicating a flatter loss region and more robust training.

E TASK-TYPE BREAKDOWN ACROSS STD/MTD/MoT

Setup and goal. We provide a consolidated evaluation on **BOBA-200** across *all* STD/MTD settings alongside MoT, covering nine benchmarks: catastrophic-forgetting-sensitive (CEV/SG/IFE), reasoning-knowledge (SQ/MP/MR), and pure reasoning (PB/LCB/GPQA-D). For each setting, we report raw scores and *group-wise average changes* versus the same-scale Base: “Avg drop (cat.)” for catastrophic-forgetting-sensitive tasks (negative indicates a drop), “Avg gain (reason.)” for reasoning-knowledge tasks, and “Avg gain (pure)” for pure reasoning tasks. We observe a trade-off among STD choices (stronger reasoning vs. better forgetting mitigation), while **MoT** simultaneously yields strong math/general reasoning gains and *significantly* mitigates catastrophic forgetting.

1134 **Summary.** Results are shown in Table 18, Table 19 and Table 20. Single-teacher choices present
 1135 a clear trade-off: some teachers maximize reasoning gains but induce larger average drops on
 1136 forgetting-sensitive tasks, while others better preserve foundational abilities but yield smaller rea-
 1137 soning gains. **MoT** alleviates this tension: it delivers strong improvements on reasoning-knowledge
 1138 and pure reasoning benchmarks, while reducing average drops on forgetting-sensitive tasks across
 1139 scales.

1140
 1141
 1142
 1143
 1144
 1145
 1146
 1147
 1148
 1149
 1150
 1151
 1152
 1153
 1154
 1155
 1156
 1157
 1158
 1159
 1160
 1161
 1162
 1163

1164 Table 18: Catastrophic-forgetting-sensitive tasks on BOBA-200 (CEV / SG / IFE). “Avg drop (cat.)”
 1165 is the average change vs. the same-scale Base (negative indicates a drop). For Qwen3-30B-A3B, SG
 1166 for $STD(QWQ)$ is unavailable (“—”); the average uses available metrics (CEV & IFE) and compares
 1167 to Base on the same subset.

1168	1169	Base model	Setting	CEV	SG	IFE	Avg drop (cat.)
1170	Qwen3-8B	Base	83.58	10.51	83.60	—	
1171		STD (Qwen3-32B)	81.35	10.38	81.34	↓1.54	
1172		STD (Qwen3-235B)	83.28	9.57	81.18	↓1.22	
1173		STD (QWQ)	83.43	9.97	81.62	↓0.89	
1174		STD (Deepseek-R1)	83.06	9.70	81.79	↓1.05	
1175		MTD (All Teachers)	83.14	10.04	82.07	↓0.81	
1176		MoT (ours)	83.73	10.15	82.04	↓0.59	
1177	Qwen3-14B	Base	86.78	10.76	84.69	—	
1178		STD (Qwen3-32B)	84.55	10.07	82.76	↓1.62	
1179		STD (Qwen3-235B)	83.73	10.26	82.56	↓1.89	
1180		STD (QWQ)	83.73	10.22	82.36	↓1.97	
1181		STD (Deepseek-R1)	84.32	9.92	82.91	↓1.69	
1182		MTD (All Teachers)	85.14	9.88	82.22	↓1.66	
1183		MoT (ours)	86.70	10.38	83.51	↓0.55	
1184	Qwen3-30B-A3B	Base	85.88	10.66	83.76	—	
1185		STD (Qwen3-32B)	85.74	9.93	82.32	↓0.77	
1186		STD (Qwen3-235B)	84.18	10.02	80.44	↓1.89	
1187		STD (QWQ)	83.80	9.65	80.03	↓2.27	
1188		STD (Deepseek-R1)	83.36	9.31	80.61	↓2.34	
1189		MTD (All Teachers)	84.55	10.12	79.77	↓1.95	
1190		MoT (ours)	86.55	10.52	83.54	↑0.10	

1188

1189 Table 19: Reasoning-related tasks on BOBA-200 (SQ / MP / MR). “Avg gain (reason.)” is the
1190 average change vs. the same-scale Base (positive indicates an increase).

Base model	Setting	SQ	MP	MR	Avg gain (reason.)
Qwen3-8B	Base	32.31	71.42	83.21	–
	STD (Qwen3-32B)	34.37	73.05	84.82	↑1.77
	STD (Qwen3-235B)	32.63	72.83	84.84	↑1.12
	STD (QWQ)	33.88	72.00	84.42	↑1.12
	STD (Deepseek-R1)	33.88	70.92	84.21	↑0.69
	MTD (All Teachers)	33.60	72.34	84.65	↑1.22
	MoT (ours)	34.44	73.30	84.42	↑1.74
Qwen3-14B	Base	32.61	75.26	85.74	–
	STD (Qwen3-32B)	32.31	75.36	85.93	↓0.00
	STD (Qwen3-235B)	32.17	74.71	86.37	↓0.12
	STD (QWQ)	32.42	74.76	85.19	↓0.41
	STD (Deepseek-R1)	32.63	74.04	86.04	↓0.30
	MTD (All Teachers)	32.77	74.97	85.82	↓0.02
	MoT (ours)	32.65	75.59	86.53	↑0.39
Qwen3-30B-A3B	Base	31.68	75.26	85.81	–
	STD (Qwen3-32B)	32.26	76.12	86.46	↑0.70
	STD (Qwen3-235B)	31.52	75.96	86.04	↑0.26
	STD (QWQ)	32.24	75.28	84.86	↓0.12
	STD (Deepseek-R1)	33.00	72.55	84.16	↓1.01
	MTD (All Teachers)	32.31	74.75	86.67	↑0.33
	MoT (ours)	32.26	76.21	86.74	↑0.82

1211

1212

1213

1214

1215

1216

1217

1218

1219

1220 Table 20: Pure reasoning tasks on BOBA-200 (PB / LCB / GPQA-D). “Avg gain (pure)” is the
1221 average change vs. the same-scale Base (positive indicates an increase).

Base model	Setting	PB	LCB	GPQA-D	Avg gain (pure)
Qwen3-8B	Base	20.47	55.76	57.77	–
	STD (Qwen3-32B)	23.19	59.06	57.42	↑1.89
	STD (Qwen3-235B)	23.17	57.90	58.11	↑1.73
	STD (QWQ)	22.85	59.88	59.85	↑2.86
	STD (Deepseek-R1)	21.90	56.78	56.50	↑0.39
	MTD (All Teachers)	22.47	54.79	60.32	↑1.19
	MoT (ours)	24.07	58.79	60.54	↑3.13
Qwen3-14B	Base	28.53	61.41	60.83	–
	STD (Qwen3-32B)	30.72	62.84	61.52	↑1.44
	STD (Qwen3-235B)	30.61	63.21	63.79	↑2.28
	STD (QWQ)	28.36	62.80	63.44	↑1.28
	STD (Deepseek-R1)	27.29	61.15	62.91	↑0.19
	MTD (All Teachers)	29.51	58.50	63.19	↑0.14
	MoT (ours)	30.77	63.59	64.26	↑2.62
Qwen3-30B-A3B	Base	28.57	61.08	59.76	–
	STD (Qwen3-32B)	33.43	61.79	60.48	↑2.10
	STD (Qwen3-235B)	33.31	61.34	61.81	↑2.35
	STD (QWQ)	32.44	60.74	60.32	↑1.36
	STD (Deepseek-R1)	29.31	59.02	59.66	↓0.47
	MTD (All Teachers)	32.50	56.85	61.33	↑0.42
	MoT (ours)	33.46	62.54	62.34	↑2.98

1242 **F DATASET**
1243
1244
1245

1246 Table 21: STD and MTD distillation datasets derived from BOBA-200 and S1K-200.

Source	Teacher	Distillation dataset name	Size
BOBA-200	QWQ	BOBA-200-QWQ	195
	Qwen3-32B	BOBA-200-32B	191
	Qwen3-235B	BOBA-200-235B	197
	Deepseek-R1	BOBA-200-R1	198
	ALL TEACHERS	BOBA-200-MTD	781
S1K-200	QWQ	S1K-200-QWQ	161
	Qwen3-32B	S1K-200-32B	164
	Qwen3-235B	S1K-200-235B	169
	Deepseek-R1	S1K-200-R1	168
	ALL TEACHERS	S1K-200-MTD	662

1260 **G ADDITIONAL TRAINING DETAILS AND FULL ABLATIONS**
12611262 **G.1 TRAINING HYPERPARAMETERS**
1263

1264 Unless otherwise noted, all experiments follow a shared set of training choices designed for long
1265 chain-of-thought (CoT) sequences and stable optimization:

- 1267 1268 • Model/input formatting: We use the Qwen3 instruction template to format prompts and
responses consistently across datasets.
- 1269 1270 • Context length: The maximum sequence length is 25k tokens to accommodate long CoT
traces with minimal truncation.
- 1271 1272 • Precision and kernels: Training uses bfloat16 with FlashAttention-2 to improve memory
efficiency and throughput for long contexts.
- 1273 1274 • Optimizer and schedule: AdamW with betas (0.9, 0.95), weight decay 0.1, cosine learning-
1275 rate schedule with a base learning rate of 1e-5 and 1% warmup. Gradients are clipped at a
1276 norm of 1.0 for stability.
- 1277 1278 • Batch and accumulation: We train on 8× H800 GPUs with a per-device batch size of 1
1279 and gradient accumulation of 8, resulting in an effective batch size of 64 sequences per
optimization step.
- 1280 1281 • Logging and checkpointing: We log every step and save a checkpoint every 50 steps; up
1282 to 10 most recent checkpoints are kept, and only model weights are saved to reduce I/O
overhead.

1283 1284 Protocol-specific details:

- 1285 1286 • MoT: One “round” consists of 50 optimization steps on a given teacher corpus before merg-
ing; we run five rounds and evaluate after each merge.
- 1287 1288 • STD/MTD: We train for 250 steps and save/evaluate checkpoints every 50 steps; the best
1289 checkpoint is reported in the main text.

1290 **G.2 STD/MTD AND MoT PER-CHECKPOINT RESULTS**
1291

1292 For STD and MTD, we train for 250 steps and save a checkpoint every 50 steps; we evaluate each
1293 checkpoint and report the best in the main text.

1294 For MoT, we alternate the base model across the four STD corpora (QWQ, Qwen3-32B, Qwen3-
1295 235B, Deepseek-R1), training 50 steps on each corpus and then performing a merge; this constitutes

1296
 1297 Table 22: Complete ablations on AIME 2024 (A24) and AIME 2025 (A25). Each entry is a 16-run
 1298 average. We report per-checkpoint results for STD/MTD (every 50 steps, up to 250), and per-round
 1299 results for MoT (Rounds 1–5).

Method	Config	BOBA-200						S1K-200					
		Qwen3-8B		Qwen3-14B		Qwen3-30B-A3B		Qwen3-8B		Qwen3-14B		Qwen3-30B-A3B	
		A24	A25	A24	A25	A24	A25	A24	A25	A24	A25	A24	A25
Base model	(40k)	75.83	67.08	79.17	70.00	81.67	72.50	75.83	67.08	79.17	70.00	81.67	72.50
STD (Qwen3-32B)	STEP 50	75.42	67.71	77.71	71.25	81.04	76.04	77.50	66.67	79.79	72.50	79.58	73.13
	STEP 100	74.17	65.83	77.71	68.13	80.83	72.50	74.58	68.96	77.71	70.21	79.58	70.63
	STEP 150	75.41	63.96	78.13	66.04	81.88	72.92	73.75	67.71	79.58	72.08	80.63	70.42
	STEP 200	74.58	63.75	76.67	66.88	80.63	75.63	75.21	66.67	79.79	69.58	79.58	70.83
	STEP 250	73.96	62.92	77.50	70.21	79.38	69.79	76.04	66.04	77.29	70.63	79.17	70.00
STD (Qwen3-235B)	STEP 50	74.58	67.92	78.13	74.79	80.00	78.13	74.38	68.54	77.92	72.71	77.92	75.63
	STEP 100	73.13	68.33	79.17	74.79	81.88	75.42	72.50	65.83	77.08	75.41	77.08	76.88
	STEP 150	71.88	66.67	78.13	70.42	77.92	76.04	74.17	67.71	77.71	72.08	78.54	74.58
	STEP 200	71.04	65.83	77.29	74.17	79.58	75.83	71.46	67.29	78.75	73.13	78.33	74.58
	STEP 250	75.00	67.29	79.38	74.17	80.42	73.54	73.96	67.08	76.67	71.46	79.17	76.04
STD (QWQ)	STEP 50	72.50	64.38	76.46	68.54	79.58	72.50	73.53	69.17	79.17	73.54	80.83	72.08
	STEP 100	75.00	67.08	78.33	73.33	78.54	76.46	76.04	68.13	79.58	71.88	81.46	72.92
	STEP 150	75.21	67.29	79.58	73.54	79.79	75.63	75.21	65.42	79.17	73.33	80.63	68.96
	STEP 200	75.83	65.83	77.29	71.46	78.54	73.96	74.58	65.63	80.21	72.92	82.08	70.63
	STEP 250	76.25	67.50	78.54	71.67	78.33	75.83	74.58	64.17	77.92	74.79	81.25	70.83
STD (Deepseek-R1)	STEP 50	67.71	60.21	74.38	67.50	78.33	68.96	70.00	61.46	73.75	62.92	78.54	70.63
	STEP 100	70.21	53.33	73.75	63.33	75.00	69.79	68.54	58.33	73.33	63.13	76.46	64.58
	STEP 150	65.83	56.04	74.58	63.75	74.79	64.38	67.92	52.08	73.96	62.71	75.63	66.04
	STEP 200	65.21	53.75	74.58	64.79	74.58	67.50	66.67	55.83	71.88	61.25	74.17	65.21
	STEP 250	66.67	55.42	72.50	63.54	75.42	66.88	66.88	51.67	72.71	63.96	74.17	70.00
MTD (ALL TEACHERS)	STEP 50	68.54	61.04	74.79	66.88	79.17	72.92	70.83	63.54	75.83	70.83	76.46	72.08
	STEP 100	73.75	66.46	76.88	72.92	79.17	73.75	75.63	70.83	78.75	73.13	77.29	75.42
	STEP 150	71.88	68.64	76.46	75.42	77.92	72.92	73.33	66.88	79.17	73.34	78.33	74.58
	STEP 200	75.00	66.04	79.58	72.50	78.75	73.75	74.17	69.38	77.08	73.33	78.33	74.58
	STEP 250	76.04	68.96	77.29	73.54	79.38	73.96	73.96	69.17	79.79	73.13	79.58	72.71
MoT (ours)	Round 1	72.29	66.88	78.75	73.95	80.63	73.13	74.79	69.17	78.33	69.79	80.00	75.42
	Round 2	75.83	69.79	79.58	73.54	79.79	76.04	77.71	70.63	80.21	74.38	82.29	74.58
	Round 3	76.67	70.42	80.00	74.79	80.00	77.92	76.25	70.00	80.00	74.38	79.79	74.79
	Round 4	78.33	70.63	79.38	76.88	81.25	75.63	77.50	71.67	79.38	75.00	80.83	77.50
	Round 5	76.45	66.88	78.96	73.75	82.92	78.33	76.25	68.13	81.67	75.63	80.00	77.50

1331 one merge round. We run five rounds in total and evaluate after every round. The complete per-round
 1332 results for all base models and both sources (BOBA-200 and S1K-200) are reported in Table 22.

1333 Key observations from the ablations:

- 1335 1. MoT consistently yields the strongest distillation gains in almost all settings.
- 1336 2. For 8B/14B bases, MTD typically surpasses the best single-teacher STD, indicating beneficial
 1337 complementarity across teachers.
- 1338 3. For 30B-A3B, MTD brings little to no gain. We hypothesize that QWQ, Qwen3-32B, and
 1339 Deepseek-R1 are not clearly stronger than the 30B base, so the union is dominated by Qwen3-235B;
 1340 in contrast, MoT can glean useful signals from the other teachers while mitigating noise, yielding
 1341 the best results.

1346 G.3 DETAILED MoT (WITHOUT R1) RESULTS ON BOBA-200

1347
 1348 Table 23 reports per-round AIME scores for MoT after ablating the Deepseek-R1 teacher (all other
 1349 settings identical). AVG is computed as the mean of AIME24 and AIME25.

1350
 1351 Table 23: MoT without Deepseek-R1 on BOBA-200: per-round AIME24/AIME25 and AVG. AVG
 1352 = (AIME24 + AIME25)/2.

Base model	Round	AIME24	AIME25	AVG
Qwen3-8B	Round 1	75.21	69.17	72.19
	Round 2	75.42	72.29	73.86
	Round 3	76.67	70.00	73.34
	Round 4	78.13	69.17	73.65
	Round 5	76.46	69.79	73.13
Qwen3-14B	Round 1	80.63	72.71	76.67
	Round 2	79.79	74.58	77.19
	Round 3	80.83	74.58	77.71
	Round 4	81.04	74.79	77.92
	Round 5	79.58	74.79	77.19
Qwen3-30B	Round 1	81.88	75.00	78.44
	Round 2	81.88	77.08	79.48
	Round 3	81.25	78.75	80.00
	Round 4	81.88	77.71	79.80
	Round 5	80.42	80.00	80.21

1370
 1371
 1372 Overall, while MoT without R1 remains competitive, the best AVG per model is consistently below
 1373 the corresponding full MoT results reported in the main text. This supports the claim that R1 offers
 1374 complementary supervision that raises the training ceiling and improves late-stage generalization.
 1375
 1376

1377 G.4 DETAILED MOT WITH PEER-LEVEL TEACHERS (QWQ + QWEN3-32B) ON BOBA-200 1378

1379 We find that teacher usefulness is not limited to strictly stronger models. Although QWQ, Qwen3-
 1380 32B, and Qwen3-30B-A3B have comparable parameter scale and reasoning performance, distilling
 1381 Qwen3-30B-A3B from peer-level teachers (QWQ or Qwen3-32B) still yields gains. This might
 1382 imply that what truly benefits the model is not necessarily higher-quality reasoning trajectories, and
 1383 reasoning trajectories distilled from peer-level teachers can still help. In addition, combining peer-
 1384 level heterogeneous trajectories with MoT further improves results, and using all teachers performs
 1385 best. Table 24 reports 16-run AIME averages on BOBA-200 with Qwen3-30B-A3B as the base.
 1386 Table 25 reports per-round AIME scores for MoT when using only peer-level teachers (QWQ and
 1387 Qwen3-32B) with Qwen3-30B as the base. AVG is computed as the mean of AIME24 and AIME25.

1388 Overall, these findings support two key conclusions:

1389 (1) Reasoning trajectories distilled from peer-level teachers can still help.
 1390 (2) MoT robustly integrates complementary and even distribution-shifted supervision, extracting
 1391 useful signals while mitigating noise.

1392
 1393
 1394 Table 24: Peer-level teachers can still help. Results on BOBA-200 with Qwen3-30B-A3B as the
 1395 base; AIME scores are 16-run averages, AVG is the mean of AIME24 and AIME25.

Teacher setting	AIME24	AIME25	AVG
Base	80.63	70.00	75.32
STD: only QWQ	79.79	75.63	77.71
STD: only Qwen3-32B	81.04	76.04	78.54
MoT: QWQ + Qwen3-32B	81.04	77.29	79.17
MoT: ALL TEACHERS	82.92	78.33	80.63

1404
 1405 Table 25: MoT with peer-level teachers (QWQ + Qwen3-32B) on BOBA-200: per-round
 1406 AIME24/AIME25 and AVG for Qwen3-30B. AVG = (AIME24 + AIME25)/2.

Round	AIME24	AIME25	AVG
Round 1	82.70	73.95	78.33
Round 2	80.83	74.58	77.71
Round 3	82.08	75.83	78.96
Round 4	80.83	75.00	77.92
Round 5	81.04	77.29	79.17

H BENCHMARK CATEGORIES AND DETAILS

We evaluate nine benchmarks under three categories—**catastrophic-forgetting-sensitive**, **reasoning-knowledge**, and **pure reasoning**—to assess whether CoT-style training with MoT preserves basic capabilities while strengthening reasoning. Here we have provided detailed content and descriptions of these tasks, and given the MoTivations for using them for evaluation and classifying them into the corresponding task categories.

H.1 CATASTROPHIC-FORGETTING-SENSITIVE TASKS

CEVAL (CEV).

Description: CEVAL is a Chinese multi-discipline multiple-choice exam suite with approximately 14,000 items spanning 52 subjects at varying difficulty levels.

Task: It evaluates factual and domain knowledge recall across humanities, sciences, and professional tracks.

MoTivation: It probes retention of broad multilingual knowledge that can degrade after CoT-style training.

SUPER.GPQA (SG).

Description: SUPER.GPQA is a graduate-level, multi-domain multiple-choice benchmark covering a wide range of academic disciplines.

Task: It measures advanced factual knowledge with light multi-step reasoning.

MoTivation: It tests whether extensive pretraining knowledge is preserved following CoT fine-tuning.

IFEVAL (IFE).

Description: IFEVAL is an instruction-following suite with automatically verifiable constraints such as length, formatting, and keyword usage.

Task: It evaluates instruction compliance and adherence to explicit constraints.

MoTivation: It checks for forgetting of fundamental alignment and compliance behaviors after CoT training.

H.2 REASONING-KNOWLEDGE TASKS

SIMPLE_QA (SQ).

Description: SIMPLE_QA is a collection of short, unambiguous fact-seeking questions with a single correct answer. *Task:* It evaluates factual accuracy and calibrated answering by discouraging uninformed guessing.

MoTivation: It tests whether CoT improves precision while avoiding hallucinations or overconfident errors.

1458 **MMLU_PRO (MP).**1459
1460 *Description:* MMLU_PRO is a harder variant of MMLU that increases item difficulty and option
1461 counts to emphasize reasoning.1462 *Task:* It measures multi-step reasoning grounded in broad subject knowledge across many domains.1463 *MoTivation:* It assesses whether CoT enhances reasoning while maintaining robust domain knowl-
1464 edge.
14651466 **MMLU_REDUX (MR).**1467
1468 *Description:* MMLU_REDUX is a curated and corrected subset of MMLU designed to reduce la-
1469 beling noise.
14701471 *Task:* It evaluates multi-subject knowledge with some analytical reasoning under cleaner annota-
1472 tions.
14731474 *MoTivation:* It isolates capability changes from dataset artifacts and checks knowledge retention
1475 under CoT.
14761477 **H.3 PURE REASONING TASKS**1478 **PhyBench (PB).**1479
1480 *Description:* PhyBench is a set of physics problems ranging from high-school to Olympiad level
1481 that require careful quantitative reasoning.
14821483 *Task:* It measures multi-step physics reasoning including derivations and the coordination of multi-
1484 ple principles.
14851486 *MoTivation:* It emphasizes chain-of-thought style reasoning rather than rote memorization of facts.
14871488 **LiveCodeBench (LCB).**1489
1490 *Description:* LiveCodeBench is a contamination-controlled suite of recent competitive program-
1491 ming problems drawn from diverse sources.
14921493 *Task:* It evaluates algorithmic reasoning, program synthesis, and debugging under executable tests.
14941495 *MoTivation:* It probes problem decomposition and step-by-step solution planning independent of
1496 encyclopedic knowledge.
14971498 **GPQA-Diamond (GPQA-D).**1499
1500 *Description:* GPQA-Diamond is the hardest expert-vetted subset of GPQA spanning biology,
1501 physics, and chemistry.
15021503 *Task:* It measures deep scientific reasoning on challenging multiple-choice questions that resist
1504 superficial lookup.
15051506 *MoTivation:* It stresses genuine multi-step reasoning and scientific insight rather than retrieval of
1507 surface facts.
15081509
1510
1511

1512
 1513 **Figure 7. Tokens marked with confidence drops in MoT under R1-distilled supervision.**
 1514 Marked tokens cluster on teacher-specific stylistic tokens while derivational tokens stay high.
 1515 This indicates that MoT attenuates inter-teacher inductive biases while preserving consensus
 1516 reasoning steps. (Note: only tokens after <|im_start|> are included in the loss.)

1517
 1518 Legend: delta_prob < -0.01 others

1519
 1520 user : Let \$ [AB CD]\$ be a convex quadrilateral with area \$ 2 0
 1521 1 4 \$, and let \$ P \$ be a point on \$ [AB]\$ and \$ Q \$
 1522 a point on \$ [AD]\$ such that triangles \$ [AB Q]\$ and \$ [AD P]\$ have area \$ 1 \$. Let \$ R \$ be the intersection of \$ [AC]\$ and \$ [PQ]\$. Determine \$ \frac{1}{2} \frac{1}{2} \$ over line \$ \{ RC \} \$ over line \$ \{ RA \} \$. Please reason step by step , and put your final
 1523 answer within \$ \boxed{\quad} \$. <|im_end|> <|im_start|> assistant <think> Alright ,
 1524 let 's tackle this geometry problem . It seems a bit complex at first , but
 1525 maybe if I break it down step by step , it will make more sense . So , we
 1526 have a convex quadrilateral ABC D with area 2 0 1 4 . There 's a point
 1527 P on side AB and a point Q on side AD such that triangles AB Q and AD P
 1528 each have area 1 . Then we need to find the ratio RC / RA where R is
 1529 the intersection of AC and PQ . First , let me visualize this quadrilateral .
 1530 Since it 's convex , all its interior angles are less than 180
 1531 degrees , and the diagonals AC and BD intersect inside the quadrilateral .
 1532 The area is given as 2 0 1 4 , which is quite large compared to the
 1533 areas of the triangles mentioned (which are 1 each) . Maybe setting up some
 1534 coordinate system would help here . Coordinates often make it easier to handle
 1535 areas and intersections . Let me try that . Suppose I place point A at the
 1536 origin (0 , 0) to simplify calculations . Let 's denote the coordinates of
 1537 B as (b , 0) since it 's on the x -axis . Similarly , point D would
 1538 then be on the y -axis , so let 's say D is (0 , d) . Since ABC D is
 1539 a convex quadrilateral , point C must be somewhere in the first quadrant .
 1540 Let me assign coordinates to C as (c , e) , where c and e are positive
 1541 numbers . So , now we have : - A : (0 , 0) - B : (b , 0)
 1542 - D : (0 , d) - C : (c , e) Now , since the quadrilateral has
 1543 an area of 2 0 1 4 , maybe I can express that in terms of the
 1544 coordinates . The area of a quadrilateral can be calculated using the shoelace
 1545 formula . Let me recall the formula for the area of a polygon with
 1546 coordinates (x 1 , y 1) , (x 2 , y 2) , ... , (x n , y n) : Area = 1
 1547 / 2 | sum from i = 1 to n of (x i * y i + 1 - x i + 1 * y i) | For
 1548 quadrilateral ABC D , plugging in the coordinates : Area = 1 / 2 | (0 * 0 + b * e + c * d + 0 * 0) - (0 * b + 0 * c + e * 0 + d * 0) | = 1 / 2 | 0 + be + cd + 0 - 0 | = 1 / 2 | be + cd | So , | be + cd | / 2 = 2 0 1 4 => be + cd = 4 0 2 8 . That will be our first equation : be + cd = 4 0 2 8 . Now , let

1560
 1561
 1562
 1563
 1564
 1565

1566
 1567 **Figure 7. Tokens marked with confidence drops in MoT under R1-distilled supervision.**
 1568 Marked tokens cluster on teacher-specific stylistic tokens while derivational tokens stay high.
 1569 This indicates that MoT attenuates inter-teacher inductive biases while preserving consensus
 1570 reasoning steps. (Note: only tokens after <|im.start|>are included in the loss.)

```

1571 's consider points P and Q . Point P is on AB , and point Q is on AD .
1572 So , param etrize their coordinates . Since AB is from ( 0 , 0 ) to ( b
1573 , 0 ), a point P on AB can be represented as ( p , 0 ) where p is
1574 between 0 and b . Similarly , AD goes from ( 0 , 0 ) to ( 0 ,d ), so
1575 Q can be represented as ( 0 , q ) where q is between 0 and d . Now ,
1576 the problem states that triangles AB Q and AD P have area 1 each . First
1577 , triangle AB Q : points A , B , Q . The coordinates are A ( 0 , 0 ),
1578 B (b , 0 ), Q ( 0 ,q ). The area can be calculated as 1 / 2 * base
1579 * height . The base AB has length b , and the height is the distance from
1580 Q to AB , which is q ( since AB is along the x -axis and Q is on the y
1581 -axis ). So area is ( 1 / 2 )* b *q = 1 . Hence , ( 1 / 2 )* b
1582 *q = 1 => b *q = 2 . Equation 2 : bq = 2 . Similarly , triangle
1583 AD P : points A , D , P . Coordinates A ( 0 , 0 ), D ( 0 ,d ), P (p
1584 , 0 ). The area can again be calculated as 1 / 2 * base * height . The
1585 base AD is length d , and the height is the distance from P to AD , which
1586 is p ( since AD is along the y -axis and P is on the x -axis ). So area
1587 is ( 1 / 2 )* d *p = 1 => d *p = 2 . Equation 3 : dp = 2 .
1588 So , from equations 2 and 3 , we have bq = 2 and dp = 2 .
1589 Therefore , we can solve for q and p : q = 2 /b and p = 2 /d . So
1590 , Q is at ( 0 , 2 /b ) and P is at ( 2 /d , 0 ). Now , we need
1591 to find the intersection point R of AC and PQ . First , let 's write
1592 equations for lines AC and PQ . Line AC connects points A ( 0 , 0 ) and C
1593 (c ,e ) . So , the param etric equations for AC can be written as x = c *t
1594 , y = e *t , where t is in [ 0 , 1 ]. Line PQ connects points P ( 2
1595 /d , 0 ) and Q ( 0 , 2 /b ). To find the equation of PQ , let 's
1596 compute the slope first . Slo pe = ( 2 /b - 0 )/ ( 0 - 2 /d ) = ( 2
1597 /b )/ ( - 2 /d ) = - d /b . So , the slope of PQ is - d /b .
1598 Therefore , the equation of PQ can be written in point -s lope form . Using
1599 point P ( 2 /d , 0 ): y - 0 = ( - d /b )( x - 2 /d ) => y =
1600 ( - d /b )x + ( d /b )( 2 /d ) => y = ( - d /b )x + 2 /b .
1601 Alternatively , using Q : y - 2 /b = ( - d /b )( x - 0 ) => y = ( - d
1602 /b )x + 2 /b . Same equation . So , equation of PQ : y = ( - d /b
1603 )x + 2 /b . Now , we need to find the intersection point R of AC and PQ
1604 . Param etrizing AC as ( ct , et ). Substitute into PQ 's equation : et
1605 = ( - d /b )( ct ) + 2 /b . So , solve for t : et = ( - cd /b )t +
1606 2 /b et + ( cd /b )t = 2 /b - t ( e + cd /b ) = 2 /b - t =
1607 ( 2 /b ) / ( e + cd /b ) = ( 2 /b ) / ( ( be + cd )/ b ) = ( 2
1608 /b ) * ( b / ( be + cd ) ) = 2 / ( be + cd ) . But earlier , we
1609 found that be + cd = 4 0 2 8 . Therefore , t = 2 / 4 0 2 8 =
1610
1611
1612
1613
1614
1615
1616
1617
1618
1619

```

1620
 1621 Figure 7. Tokens marked with confidence drops in MoT under R1-distilled supervision.
 1622 Marked tokens cluster on teacher-specific stylistic tokens while derivational tokens stay high.
 1623 This indicates that MoT attenuates inter-teacher inductive biases while preserving consensus
 1624 reasoning steps. (Note: only tokens after <|im.start|>are included in the loss.)

```

1625 1 / - 2 0 1 4 . Therefore , the coordinates of R are ( c * t , e * t
1626 ) = ( c / 2 0 1 4 , e / 2 0 1 4 ). So , R divides AC such that RA
1627 is the distance from A to R , and RC is from R to C . Since AC is
1628 parameter ized by t from 0 to 1 , with t = 0 at A and t = 1 at C
1629 , the ratio RC / RA is ( 1 - t )/ t . But in this case , t is 1 /
1630 2 0 1 4 . Therefore , RC / RA = ( 1 - 1 / 2 0 1 4 ) / ( 1 / 2
1631 0 1 4 ) ) = ( 2 0 1 3 / 2 0 1 4 ) / ( 1 / 2 0 1 4 ) ) = 2
1632 0 1 3 . Hence , the ratio is 2 0 1 3 . Wait , so the answer is 2
1633 0 1 3 ? That seems plausible . Let me check my steps again to be sure . 1
1634 . Set coordinates for the quadrilateral with A at ( 0 , 0 ), B (b , 0
1635 ), D ( 0 ,d ), C (c ,e ). Correct . 2 . Calculated area using shoelace
1636 formula : got be + cd = 4 0 2 8 . Seems right . 3 . Found points
1637 P ( 2 /d , 0 ) and Q ( 0 , 2 /b ). Yes , based on the area
1638 conditions . 4 . Equation for PQ : derived slope - d /b and equation y =
1639 (- d /b )x + 2 /b . Check . 5 . Parameterizing AC as ( ct , et )
1640 and solving for intersection . Found t = 1 / 2 0 1 4 . Then , RA is
1641 the distance from A to R : since R is at t = 1 / 2 0 1 4 , RA
1642 corresponds to t = 1 / 2 0 1 4 , and RC is the remaining distance from
1643 R to C : 1 - t . Therefore , ratio RC / RA = ( 1 - t )/ t = ( 1
1644 - 1 / 2 0 1 4 )/ ( 1 / 2 0 1 4 ) = ( 2 0 1 3 / 2 0 1 4 )/ ( 1
1645 / 2 0 1 4 ) = 2 0 1 3 . So yes , seems correct . Alternatively ,
1646 since coordinates are linear , t is the parameter along AC , so the ratios
1647 are related directly to the parameter t . So another way : RA : RC = t :
1648 ( 1 - t ) , so RC / RA = ( 1 - t )/ t = ( 1 / ( t ) ) - 1 .
1649 Since t = 1 / 2 0 1 4 , RC / RA = 2 0 1 4 - 1 = 2 0 1 3 .
1650 Perfect . Therefore , the final answer is 2 0 1 3 . Pretty elegant !
1651 Using coordinates made it straightforward , even if setting up the coordinates
1652 took some time . Let me just think if there 's any other way without
1653 coordinates , but perhaps this is the most direct method here . ** Final
1654 Answer ** \boxed { 2 0 1 3 } </think> Given a convex quadrilateral \(
1655 AB CD \) with area 2 0 1 4 , points \ ( P \) on \ ( AB \) and \ ( Q \)
1656 on \ ( AD \) are such that triangles \ ( AB Q \) and \ ( AD P \) each have
1657 area 1 . We need to determine the ratio \ ( \frac { 1 } { \text{line} \{ RC \} } )
1658 \ ( \text{line} \{ RA \} ) \) where \ ( R \) is the intersection of \ ( AC \) and
1659 \ ( P Q \) . 1 . ** Coordinate Setup ** : - Place \ ( A \) at \ ( 0
1660 , 0 \) , \ ( B \) at \ ( b , 0 \) , \ ( D \) at \ ( 0 , d \)
1661 \) , and \ ( C \) at \ ( c , e \) . - The area of \ ( AB CD \) is
1662 given by the shoelace formula , leading to the equation \ ( be + cd = 4
1663 0 2 8 \) . 2 . ** Points \ ( P \) and \ ( Q \) ** : - \ ( P \) on
1664
1665
1666
1667
1668
1669
1670
1671
1672
1673
```

1674
1675
1676
1677
1678

Figure 7. Tokens marked with confidence drops in MoT under R1-distilled supervision.
Marked tokens cluster on teacher-specific stylistic tokens while derivational tokens stay high.
This indicates that MoT attenuates inter-teacher inductive biases while preserving consensus
reasoning steps. (Note: only tokens after <|im.start|> are included in the loss.)

1679
1680
1681
1682
1683
1684
1685
1686
1687
1688
1689
1690
1691
1692
1693
1694
1695
1696
1697

```
\( AB \) is \(( p , 0 )\ ) and \(\( Q \) on \(\( AD \) is \(( 0 , q )\ ). - Areas of triangles \(\( AB Q \) and \(\( AD P \) are 1 , leading to \(\( b q = 2 \) and \(\( dp = 2 \). Thus , \(\( q = \frac{2}{b} ) and \(\( p = \frac{2}{d} ). 3 . ** Equations of Lines ** : - Line \(\( P Q \) has slope \(\( - \frac{d}{b} ) and equation \(\( y = - \frac{d}{b} x + \frac{2}{b} ). - Line \(\( AC \) is parameterized as \(\( x = ct \) and \(\( y = et \) for \(\( t \) in [ 0 , 1 ]. 4 . ** Intersection Point \(\( R \) ** : - Substitute the parametric coordinates of \(\( AC \) into the equation of \(\( P Q \): \(\( et = - \frac{d}{b} ct + \frac{2}{b} ). - Solving for \(\( t \) gives \(\( t = \frac{b + cd}{d - 2b} ). 5 . ** Ratio Calculation ** : - The coordinates of \(\( R \) are \(\( \left( \frac{c}{2} , \frac{e}{2} \right) \). - The ratio \(\( \frac{RC}{RA} \) is \(\( \frac{1 - t}{t} ) = \frac{1}{2} . 1 3 \). \(\boxed{2} <|im_end|>
```

1698
1699
1700
1701
1702
1703
1704
1705
1706
1707
1708
1709
1710
1711
1712
1713
1714
1715
1716
1717
1718
1719
1720
1721
1722
1723
1724
1725
1726
1727

1728
1729
1730
1731
1732
1733
1734
1735

Figure 8. Tokens marked with confidence drops in STD(R1) under R1-distilled supervision. Marked tokens are rare to nearly absent, indicating that direct distillation fully adopts the teacher’s trajectory, including stylistic tokens and latent inductive biases, rather than filtering them. (Note: only tokens after <|im_start|> are included in the loss.)

Legend: delta_prob < -0.01 others

1736 user Let \$ [AB CD]\$ be a convex quadrilateral with area \$ 2 0
1737 1 4 \$, and let \$ P \$ be a point on \$ [AB]\$ and \$ Q \$
1738 a point on \$ [AD]\$ such that triangles \$ [AB Q]\$ and \$ [\$
1739 \$ AD P]\$ have area \$ 1 \$. Let \$ R \$ be the intersection of \$ [\$
1740 \$ AC]\$ and \$ [P Q]\$. Determine \$ \frac{1}{2} \frac{1}{2} \$ over line \$ \{ RC \} \$ \$ \{ \$
1741 over line \$ \{ RA \} \$ \$. Please reason step by step , and put your final
1742 answer within \$ \boxed{ } \$. <|im_end|> <|im_start|> assistant > <think> Alright ,
1743 let 's tackle this geometry problem . It seems a bit complex at first , but
1744 maybe if I break it down step by step , it will make more sense . So , we
1745 have a convex quadrilateral ABC D with area 2 0 1 4 . There 's a point
1746 P on side AB and a point Q on side AD such that triangles AB Q and AD P
1747 each have area 1 . Then we need to find the ratio RC / RA where R is
1748 the intersection of AC and PQ . First , let me visualize this quadrilateral .
1749 Since it 's convex , all its interior angles are less than 180
1750 degrees , and the diagonals AC and BD intersect inside the quadrilateral .
1751 The area is given as 2 0 1 4 , which is quite large compared to the
1752 areas of the triangles mentioned (which are 1 each) . Maybe setting up some
1753 coordinate system would help here . Coordinates often make it easier to handle
1754 areas and intersections . Let me try that . Suppose I place point A at the
1755 origin (0 , 0) to simplify calculations . Let 's denote the coordinates of
1756 B as (b , 0) since it 's on the x -axis . Similarly , point D would
1757 then be on the y -axis , so let 's say D is (0 , d) . Since ABC D is
1758 a convex quadrilateral , point C must be somewhere in the first quadrant .
1759 Let me assign coordinates to C as (c , e) , where c and e are positive
1760 numbers . So , now we have : - A : (0 , 0) - B : (b , 0)
1761 - D : (0 , d) - C : (c , e) Now , since the quadrilateral has
1762 an area of 2 0 1 4 , maybe I can express that in terms of the
1763 coordinates . The area of a quadrilateral can be calculated using the shoelace
1764 formula . Let me recall the formula for the area of a polygon with
1765 coordinates (x 1 , y 1) , (x 2 , y 2) , ... , (x n , y n) : Area = 1
1766 / 2 | sum from i = 1 to n of (x i * y i + 1 - x i + 1 * y i) | For
1767 quadrilateral ABC D , plugging in the coordinates : Area = 1 / 2 | (0 * 0 + b * e + c * d + 0 * 0) - (0 * b + 0 * c + e * 0 + d * 0) | = 1 / 2 | 0 + be + cd + 0 - 0 | = 1 / 2 | be + cd | So , | be + cd | / 2 = 2 0 1 4 => be + cd = 4 0 2 8 . That will be our first equation : be + cd = 4 0 2 8 . Now , let

1776
1777
1778
1779
1780
1781

1782
1783
1784
1785
1786

Figure 8. Tokens marked with confidence drops in STD(R1) under R1-distilled supervision. Marked tokens are rare to nearly absent, indicating that direct distillation fully adopts the teacher's trajectory, including stylistic tokens and latent inductive biases, rather than filtering them. (Note: only tokens after <|im_start|> are included in the loss.)

```
's consider points P and Q . Point P is on AB , and point Q is on AD .  
So , parametrize their coordinates . Since AB is from ( 0 , 0 ) to ( b , 0 ), a point P on AB can be represented as ( p , 0 ) where p is between 0 and b . Similarly , AD goes from ( 0 , 0 ) to ( 0 , d ), so Q can be represented as ( 0 , q ) where q is between 0 and d . Now , the problem states that triangles ABQ and ADP have area 1 each . First , triangle ABQ : points A , B , Q . The coordinates are A ( 0 , 0 ), B ( b , 0 ), Q ( 0 , q ). The area can be calculated as 1 / 2 * base * height . The base AB has length b , and the height is the distance from Q to AB , which is q ( since AB is along the x -axis and Q is on the y -axis ). So area is ( 1 / 2 ) * b * q = 1 . Hence , ( 1 / 2 ) * b * q = 1 => b * q = 2 . Equation 2 : bq = 2 . Similarly , triangle ADP : points A , D , P . Coordinates A ( 0 , 0 ), D ( 0 , d ), P ( p , 0 ). The area can again be calculated as 1 / 2 * base * height . The base AD is length d , and the height is the distance from P to AD , which is p ( since AD is along the y -axis and P is on the x -axis ). So area is ( 1 / 2 ) * d * p = 1 => d * p = 2 . Equation 3 : dp = 2 . So , from equations 2 and 3 , we have bq = 2 and dp = 2 . Therefore , we can solve for q and p : q = 2 / b and p = 2 / d . So , Q is at ( 0 , 2 / b ) and P is at ( 2 / d , 0 ). Now , we need to find the intersection point R of AC and PQ . First , let 's write equations for lines AC and PQ . Line AC connects points A ( 0 , 0 ) and C ( c , e ). So , the parametric equations for AC can be written as x = c * t , y = e * t , where t is in [ 0 , 1 ]. Line PQ connects points P ( 2 / d , 0 ) and Q ( 0 , 2 / b ). To find the equation of PQ , let 's compute the slope first . Slope = ( 2 / b - 0 ) / ( 0 - 2 / d ) = ( 2 / b ) / ( - 2 / d ) = - d / b . So , the slope of PQ is - d / b . Therefore , the equation of PQ can be written in point-slope form . Using point P ( 2 / d , 0 ): y - 0 = ( - d / b )( x - 2 / d ) => y = ( - d / b )x + ( d / b )( 2 / d ) => y = ( - d / b )x + 2 / b . Alternatively , using Q : y - 2 / b = ( - d / b )( x - 0 ) => y = ( - d / b )x + 2 / b . Same equation . So , equation of PQ : y = ( - d / b )x + 2 / b . Now , we need to find the intersection point R of AC and PQ . Parametrizing AC as ( ct , et ). Substitute into PQ 's equation : et = ( - d / b )( ct ) + 2 / b . So , solve for t : et = ( - cd / b )t + 2 / b - et + ( cd / b )t = 2 / b - t ( e + cd / b ) = 2 / b - t = ( 2 / b ) / ( e + cd / b ) = ( 2 / b ) / ( ( be + cd ) / b ) = ( 2 / b ) * ( b / ( be + cd ) ) = 2 / ( be + cd ) . But earlier , we found that be + cd = 4 0 2 8 . Therefore , t = 2 / 4 0 2 8 =
```

1830
1831
1832
1833
1834
1835

Figure 8. Tokens marked with confidence drops in STD(R1) under R1-distilled supervision. Marked tokens are rare to nearly absent, indicating that direct distillation fully adopts the teacher’s trajectory, including stylistic tokens and latent inductive biases, rather than filtering them. (Note: only tokens after <|im_start|> are included in the loss.)

1 / 2 0 1 4 . Therefore , the coordinates of R are (c * t , e * t) = (c / 2 0 1 4 , e / 2 0 1 4). So , R divides AC such that RA is the distance from A to R , and RC is from R to C . Since AC is parameter ized by t from 0 to 1 , with t = 0 at A and t = 1 at C , the ratio RC / RA is (1 - t)/ t . But in this case , t is 1 / 2 0 1 4 . Therefore , RC / RA = (1 - 1 / 2 0 1 4) / (1 / 2 0 1 4) = (2 0 1 3 / 2 0 1 4) / (1 / 2 0 1 4) = 2 0 1 3 . Hence , the ratio is 2 0 1 3 . Wait , so the answer is 2 0 1 3 ? That seems plausible . Let me check my steps again to be sure . 1 . Set coordinates for the quadrilateral with A at (0 , 0), B (b , 0), D (0 ,d), C (c ,e). Correct . 2 . Calculated area using shoelace formula : got be + cd = 4 0 2 8 . Seems right . 3 . Found points P (2 /d , 0) and Q (0 , 2 /b). Yes , based on the area conditions . 4 . Equation for PQ : derived slope = d /b and equation y = (- d /b)x + 2 /b . Check . 5 . Parameterizing AC as (ct , et) and solving for intersection . Found t = 1 / 2 0 1 4 . Then , RA is the distance from A to R : since R is at t = 1 / 2 0 1 4 , RA corresponds to t = 1 / 2 0 1 4 , and RC is the remaining distance from R to C : 1 - t . Therefore , ratio RC / RA = (1 - t)/ t = (1 - 1 / 2 0 1 4)/ (1 / 2 0 1 4) = (2 0 1 3 / 2 0 1 4)/ (1 / 2 0 1 4) = 2 0 1 3 . So yes , seems correct . Alternatively , since coordinates are linear , t is the parameter along AC , so the ratios are related directly to the parameter t . So another way : RA : RC = t : (1 - t) , so RC / RA = (1 - t)/ t = (1 / (t)) - 1 . Since t = 1 / 2 0 1 4 , RC / RA = 2 0 1 4 - 1 = 2 0 1 3 . Perfect . Therefore , the final answer is 2 0 1 3 . Pretty elegant ! Using coordinates made it straightforward , even if setting up the coordinates took some time . Let me just think if there 's any other way without coordinates , but perhaps this is the most direct method here . ** Final Answer ** \boxed{2 0 1 3} </think> Given a convex quadrilateral \(\triangle ABCD\) with area 2 0 1 4 , points \(\triangle P\) on \(\triangle AB\) and \(\triangle Q\) on \(\triangle AD\) are such that triangles \(\triangle ABQ\) and \(\triangle ADP\) each have area 1 . We need to determine the ratio \(\frac{RC}{RA}\) where \(\triangle R\) is the intersection of \(\triangle AC\) and \(\triangle PQ\). 1 . ** Coordinate Setup ** : - Place \(\triangle A\) at \((0, 0)\), \(\triangle B\) at \((b, 0)\), \(\triangle D\) at \((0, d)\), and \(\triangle C\) at \((c, e)\) . - The area of \(\triangle ABCD\) is given by the shoelace formula , leading to the equation be + cd = 4 0 2 8 . 2 . ** Points \(\triangle P\) and \(\triangle Q\)** : - \(\triangle P\) on

1890
1891
1892
1893
1894

Figure 8. Tokens marked with confidence drops in STD(R1) under R1-distilled supervision. Marked tokens are rare to nearly absent, indicating that direct distillation fully adopts the teacher’s trajectory, including stylistic tokens and latent inductive biases, rather than filtering them. (Note: only tokens after <|im_start|> are included in the loss.)

```
1895 \(\ AB \backslash \) is \((\ p \ , \ 0 \ )\ \ ) and \(\ Q \backslash \) on \(\ AD \backslash \) is \((\ 0 \ , \ 
1896 q \ )\ \ ). - Areas of triangles \(\ AB \ Q \backslash \) and \(\ AD \ P \backslash \) are \ 1 \ , 
1897 leading to \(\ b \ q = 2 \ \ ) and \(\ dp = 2 \ \ ). Thus , \(\ q = \frac{2}{b} \ 
1898 \{ 2 \} \{ b \} \ ) and \(\ p = \frac{2}{d} \ 
1899 \{ 2 \} \{ d \} \ ). 3 . ** Equations of 
1900 Lines ** : - Line \(\ P \ Q \backslash \) has slope \(- \frac{d}{b} \ 
1901 and equation \(\ y = - \frac{d}{b} x + \frac{2}{b} \ 
1902 Line \(\ AC \backslash \) is parameterized as \(\ x = ct \) and \(\ y = et \) for \(\ 
1903 t \in [0 , 1] \ ). 4 . ** Intersection Point \(\ R \backslash \) ** : - 
1904 Substitute the parametric coordinates of \(\ AC \backslash \) into the equation of \(\ P 
1905 Q \backslash \ ): \ et = - \frac{d}{b} ct + \frac{2}{b} 
1906 \ ] - Solving for \(\ t \) gives \(\ t = \frac{b + cd}{d - 2b} \ 
1907 = \frac{1}{2} \{ 2 \ 0 \ 1 \ 4 \} \ ). 5 . ** Ratio Calculation ** : - The 
1908 coordinates of \(\ R \backslash \) are \(\ (\left( \frac{c}{2} \ 0 \ 1 \ 4 \right), \frac{e}{2} \{ 2 \ 0 \ 1 \ 4 \} \) right) \). - The ratio \(\ (\frac{c}{2} \ 0 \ 1 \ 4 \) over line \{ 
1909 RC \} \) \ over line \{ RA \} \) is \(\ (\frac{1 - t}{t} \) = \(\frac{1}{2} \{ 1 \ 3 \} \) = \(\frac{1}{2} \ 0 \ 
1910 1 \ 3 \ \ ). \ [ \boxed{2 \ 0 \ 1 \ 3} \ ] <|im_end|> 
1911 
1912 
1913 
1914 
1915 
1916 
1917 
1918 
1919 
1920 
1921 
1922 
1923 
1924 
1925 
1926 
1927 
1928 
1929 
1930 
1931 
1932 
1933 
1934 
1935 
1936 
1937 
1938 
1939 
1940 
1941 
1942 
1943
```

1944
1945

THE USE OF LARGE LANGUAGE MODELS (LLMs)

1946
1947
1948
1949
1950
1951
1952
1953

We used large language models (LLMs) as general-purpose assist tools for editing (English proof-reading, minor wording/LaTeX refactoring) and for generating figure/table captions drafts that were subsequently verified and rewritten by the authors. LLMs did not design experiments, select results, write the core method, or generate evaluation numbers. All experimental outputs, metrics, and plots derive from our released code and logs. Separately, the research subject of this paper employs teacher LLMs to produce chains-of-thought for distillation; this is part of the method under study, not assistance in authorship. The authors take full responsibility for the content and have verified factual claims and citations. No text was copied from third-party sources without attribution.

1954
1955
1956
1957
1958
1959
1960
1961
1962
1963
1964
1965
1966
1967
1968
1969
1970
1971
1972
1973
1974
1975
1976
1977
1978
1979
1980
1981
1982
1983
1984
1985
1986
1987
1988
1989
1990
1991
1992
1993
1994
1995
1996
1997